

Supporting information for

Importance of the curvature in electronic, structural and charge transport properties: Oligomers of *N*-pyridine carbazole

Clément Brouillac,^a Ari Serez,^b Nemo McIntosh,^b Joëlle Rault-Berthelot,^a Olivier Jeannin,^a Benoît Heinrich,^c Cassandre Quinton,^a Olivier De Sagazan,^d Emmanuel Jacques,^d Jérôme Cornil,^b and Cyril Poriel^{a*}

^a Univ Rennes, CNRS, ISCR-UMR 6226, F-35000 Rennes, France, ^b Laboratory for Chemistry of Novel Materials, University of Mons, Mons, Belgium, ^c Institut de Physique et Chimie des Matériaux de Strasbourg, UMR 7504, CNRS-Université de Strasbourg, 67034 Strasbourg Cedex 2, France, ^d Univ Rennes, CNRS, IETR-UMR 6164, F-35000 Rennes, France,

email: cyril.poriel@univ-rennes.fr

1	General information.....	3
1.1	Synthesis.....	3
1.2	Spectroscopic studies	3
1.3	X-ray.....	4
1.4	Electrochemical studies.....	4
1.5	Molecular modelling	5
1.6	Atomic force microscopy measurement.....	5
1.7	Devices fabrication and characterization	5
2	Synthetic procedures.....	7
2.1	General procedure for Ullmann coupling reaction.....	7
2.2	2,7-dibromo-9-(pyridin-2-yl)-9H-carbazole (1).....	8
2.3	2-bromo-9-(pyridin-2-yl)-9H-carbazole (2).....	8
2.4	9-(pyridin-2-yl)-2-(4,4,5,5-tetramethyl-1,3,2-dioxaborolan-2-yl)-9H-carbazole (3)....	9
2.5	7-bromo-9,9'-di(pyridin-2-yl)-9H,9'H-2,2'-bicarbazole (4)	9
2.6	9,9',9",9""-tetra(pyridin-2-yl)-9H,9'H,9" H,9""H-2,2':7',2":7",2""-quatercarbazole ([4]L-Py-Cbz)	10
3	Photophysical properties.....	11
4	Electrochemical properties	16
5	Molecular modelling.....	17
6	Structural properties.....	42
6.1	Displacement angle	42
6.2	Torsion angle.....	43
6.3	Dihedral angle between carbazole and substituent	44
6.4	Torsion angle between two carbazoles at S ₀ from optimized structures of [4]C-Py-Cbz and [4]L-Py-Cbz (B3LYP/6-31+g(d))	44
6.5	Torsion angle between two carbazoles at S ₁ from optimized structures of [4]C-Py-Cbz and [4]L-Py-Cbz (B3LYP/6-31+g(d))	45
7	Organic field effect transistor and space-charged-limited current diode measurements ...	45
8	Atomic Force Microscopy measurement.....	46
9	Thermal properties	47
10	X-Ray parameters	48
11	Copy of NMR Spectra	50
12	Copy of mass spectra	65
13	References.....	69

1 General information

1.1 Synthesis

All manipulations of oxygen and moisture-sensitive materials were conducted with a standard Schlenk technique. All glassware was kept in an oven at 80°C. Argon atmosphere was generated by three repetitive cycles of vacuum/Argon using a Schlenk ramp. Commercially available reagents and solvents were used without further purification other than those detailed below. THF was obtained through a PURE SOLV™ solvent purification system. Light petroleum refers to the fraction with bp 40-60°C. The ultrapure water had a resistivity of 18.2 MΩ cm (Purelab Classic UV). Analytical thin layer chromatography was carried out using aluminum backed plates coated with Merck Kieselgel 60 GF254 and visualized under UV light (at 254 and 360 nm). Flash chromatography was carried out using Teledyne Isco CombiFlash® Rf 400 (UV detection 200-360nm) or Teledyne Isco CombiFlash Nextgen 300+ (UV detection 200-360 nm), over standard silica cartridges (Redisep® Isco or Puriflash® columns Interchim).¹H and ¹³C NMR spectra were recorded using Bruker 300 MHz instruments (¹H frequency, corresponding ¹³C frequency: 75 MHz); chemical shifts were recorded in ppm and J values in Hz. The residual signals for the NMR solvents used are 5.32 ppm (proton) and 54.00 ppm (carbon) for CD₂Cl₂ and 7.26 ppm (proton) and 77,16 ppm (carbon) for CDCl₃.¹ The following abbreviations have been used for the NMR assignment: s for singlet, d for doublet, t for triplet, q for quadruplet and m for multiplet. High resolution mass spectra were recorded at the Centre Régional de Mesures Physiques de l'Ouest (CRMPO-Rennes) on a Thermo Fisher Q-Exactive instrument or a Bruker MaXis 4G or a Bruker Ultraflex III.

1.2 Spectroscopic studies

Dichloromethane (spectroscopic grade, Acros), 2-MeTHF (spectroscopic grade, Sigma Aldrich), 1 N solution of sulfuric acid in water (Standard solution, Alfa Aesar), and quinine sulfate dihydrate (99+, ACROS organics) were used without further purification.

UV-visible spectra were recorded using an UV-Visible spectrophotometer JASCO-V630BIO. Emission spectra were recorded with a HORIBA Scientific Fluoromax-4 equipped with a Xenon lamp for fluorescence measurement. Emission spectra were recorded with a JASCO FP-8300 for phosphorescence measurement with a delay of 10 ms to remove the fluorescence contribution. Triplet energy levels were calculated from the first peak of the phosphorescence spectrum at 77 K. Conversion in electron-volt was obtained with the following formula:

$$E(eV) = \frac{h\nu}{\lambda}$$

with $h = 6.62607 \times 10^{-34}$ J.s, $C = 2.99792 \times 10^{17}$ nm.s⁻¹ and $1 \text{ eV} = 1.60218 \times 10^{-19}$ J. This equation can be simplified as:

$$E(eV) = \frac{1239.84}{\lambda}$$

with λ formulated in nm.

Quantum yields in solution (QYsol) were calculated relative to quinine sulfate (QYref = 0.546 in H₂SO₄ 1 N). QYsol was determined according to the following equation,

$$QY_{sol} = QY_{ref} \times \frac{Grad_s}{Grad_r} \times \left(\frac{\eta_s}{\eta_r} \right)^2$$

where subscripts *s* and *r* refer respectively to the sample and reference, *Grad* is the gradient from the plot of integrated fluorescence intensity vs absorbance, η is the refracting index of the solvent ($\eta_s = 1.421$ for dichloromethane). Four solutions of different concentration ($A < 0.1$) of the sample and five solutions of the reference (quinine sulfate) were prepared. The integrated area of the fluorescence peak was plotted against the absorbance at the excitation wavelength for both the sample and reference. The gradients of these plots were then injected in the equation to calculate the reported quantum yield value for the sample.

Absolute quantum yields of the films were recorded using a deported HORIBA Scientific Quanta-Phi integrating sphere linked to the Fluoromax-4.

Emission decay measurements were carried out on the HORIBA Scientific Fluoromax-4 equipped with its TCSPC pulsed source interface.

Spin-coated films were prepared from a 1mg/mL in THF solution using a Labspins Tournette from Süss Microtec.

1.3 X-ray

Crystals were picked up with a cryoloop and then frozen at 150 K under a stream of dry N₂. Data were collected on a D8 VENTURE Bruker AXS diffractometer with Mo-K α radiation ($\lambda = 0.71073 \text{ \AA}$).

Structures were solved by direct methods (SIR92)² and refined (SHELXL-2014/7)³ by full-matrix least-squares methods as implemented in the WinGX software package.⁴ An empirical absorption (multi-scan) correction was applied. Hydrogen atoms were introduced at calculated positions (riding model) included in structure factor calculation but not refined. Refinement parameters are summarized in Table S14 and Table S15.

Crystallographic data have been deposited with the Cambridge Crystallographic Data Centre as supplementary publication data: [4]C-Py-Cbz (CCDC 2265379), [4]L-Py-Cbz (CCDC 2325120). Copies of the data can be obtained free of charge on application to CCDC, 12 Union Road, Cambridge CB2 1EZ, UK [fax: (+44) 1223-336-033; e-mail: deposit@ccdc.cam.ac.uk].

Figures were generated with Mercury software 3.9.

1.4 Electrochemical studies

Electrochemical experiments were performed under argon atmosphere using a Pt disk electrode (diameter 1 mm). The counter electrode was a vitreous carbon rod. The reference electrode was either a silver wire in a 0.1 M AgNO₃ solution in CH₃CN for the studies in oxidation or a Silver wire coated by a thin film of AgI (silver(I)iodide) in a 0.1 M Bu₄NI solution in DMF for the studies in reduction. Ferrocene was added to the electrolyte solution at the end of a series of experiments. The ferrocene/ferrocenium (Fc/Fc⁺) couple served as internal standard. The three electrodes cell was connected either to a PAR Model 273 potentiostat/galvanostat (PAR, EG&G, USA) monitored with the ECHEM Software or to a potentiostat/galvanostat (Autolab/PGSTAT101) monitored with the Nova 2.1 Software. Activated Al₂O₃ was added in the electrolytic solution to remove excess moisture. For a further comparison of the electrochemical and optical properties, all potentials are referred to the SCE electrode that was calibrated at - 0.405 V vs. Fc/Fc⁺ system. Following the work of Jenekhe,⁵ we estimated the electron affinity (EA) or lowest unoccupied molecular orbital (LUMO) and the ionization potential (IP) or highest occupied molecular orbital (HOMO) from the redox data. The LUMO level was calculated from: LUMO (eV) = -[E_{onset}^{red} (vs SCE) + 4.4]. Similarly the HOMO level was calculated from: HOMO (eV) = -[E_{onset}^{ox} (vs SCE) + 4.4], based on a SCE energy level of

4.4 eV relative to the vacuum. The electrochemical gap was calculated from: $\Delta E^{\text{el}} = |\text{HOMO-LUMO}|$ (in eV).

1.5 Molecular modelling

Geometry optimization of the fundamental state (S_0) was performed using Density Functional Theory (DFT) calculations using the B3LYP functional and the 6-31G(d) basis set. All stationary points were characterized as minima by analytical frequency calculations.

Optical transition diagrams were obtained through TD-DFT calculations performed using the B3LYP functionals and the 6-311+G(d,p) basis set from the geometry of S_0 .

Geometry optimization of the first excited singlet state (S_1) was performed using Density Functional Theory (DFT) calculations using the B3LYP functional and the 6-31+G(d,p) basis set.

This work was granted access to the HPC resources of TGCC/CEA/CINES/IDRIS under the allocation 2024 AD010814136R1 awarded by GENCI. Figures were generated with GaussView 6.0 and GaussSum 3.0.

1.6 Atomic force microscopy measurement

AFM images were recorded on the Bruker Multimode 8 using PeakForce Tapping with a resolution of 512 x 512 pixels on a 500nm x 500nm surface. Scan rate has been set at 1 Hz. Each scan line in the image was scanned from left to right (trace) and from right to left (retrace). The observed topographic features were verified for their consistency between trace and retrace images. Amplitude set point was set to 1.68 mV and the drive amplitude was set to 10.38 mV. Roughness has been extracted from these images using Nano Scope Analysis 1.8 after a clean image treatment.

1.7 Devices fabrication and characterization

Organic field effect transistors (OFETs)

The fabrication process is described as follows: 150 nm thick aluminium layer was evaporated and patterned by conventional photolithography on $5 \times 5 \text{ cm}^2$ rigid glass substrate. Then, SU-8 2000.5 Photoresist from Microchem⁶ was then spin-coated in order to obtain a 400 nm thick layer. 50 nm thick gold layer was then thermally evaporated and patterned by photolithography. Finally, the OSCs were deposited by evaporation under vacuum as a 40 nm thick layer.

Current/voltage characteristics:

The evaluation of carrier mobility has been made using the transistor structure without applying any gate-source voltage. Thus, lateral current between drain and source has been measured according to drain-source voltage.

Transfer Characteristics:

The transfer characteristics correspond to the measurement of drain current I_D as a function of gate-source voltage V_{GS} at constant drain-source voltage V_{DS} . Current drain is represented in logarithmic scale. This measurement is carried out with low and high V_{DS} corresponding to linear and saturated regimes of the OFET. These measurements have been carried out using Keithley semiconductor characterization system 2636a.

Field effect mobility: In the linear regime ($V_{DS} \leq V_{GS} - V_{TH}$), the drain current I_D is given by:

$$I_D = \frac{WC_i}{L} \mu_{FE_Lin} (V_{GS} - V_{TH}) V_{DS}$$

Where W and L are the channel width and length, respectively. C_i is the capacitance per unit area of the insulator, μ_{FE_lin} is the field-effect mobility in the linear regime, respectively. V_{GS} and V_{DS} are the gate-source voltage and drain-source voltage, respectively. V_{TH} is the threshold voltage. Field-effect mobility in the linear regime can be expressed by:

$$\mu_{FE_Lin} = \frac{L}{WC_i V_{DS}} \frac{\partial I_D}{\partial V_{GS}}$$

To evaluate the field-effect mobility in the saturation regime ($V_{DS} \geq V_{GS} - V_{TH}$), the drain current I_D is given by:

$$I_D = \frac{WC_i}{L} \mu_{FE_Sat} (V_{GS} - V_{TH})^2$$

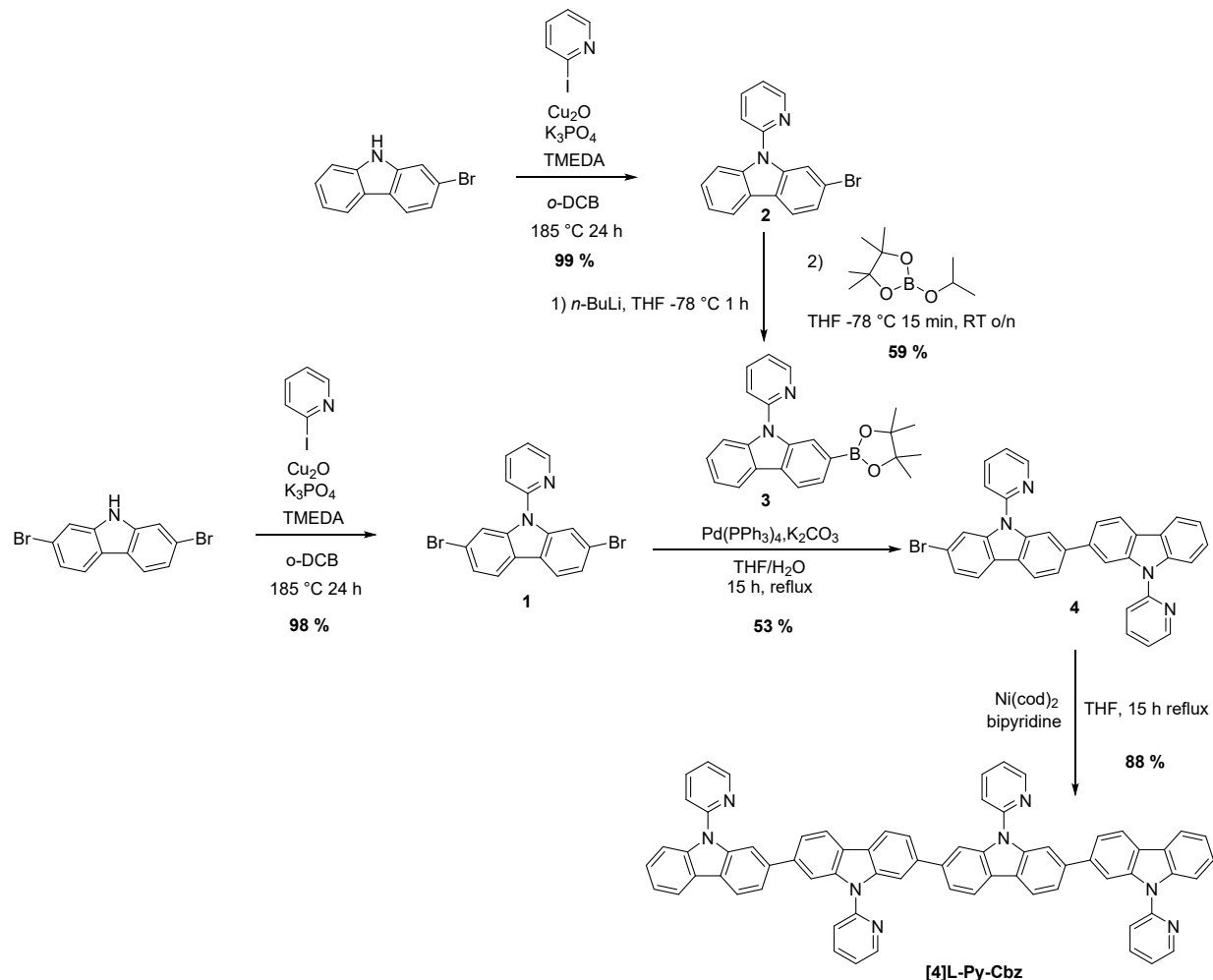
Field-effect mobility in the saturation regime can be expressed by:

$$\mu_{FE_Sat} = \frac{2L}{WC_i} \left(\frac{\partial \sqrt{I_D}}{\partial V_{GS}} \right)_2$$

2 Synthetic procedures

The synthesis of [4]C-Py-Cbz is reported elsewhere.⁷ All relevant information for synthetic procedures and characterization can be found in the literature.⁷

The synthesis of [4]L-Py-Cbz is presented below.

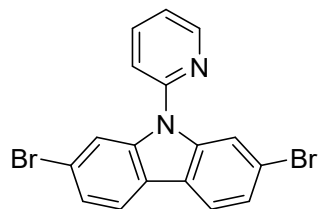


Scheme S 1 Synthesis pathway of [4]L-Py-Cbz

2.1 General procedure for Ullmann coupling reaction.

2,7-Dibromo-9H-carbazole (1.0 eq), pyridine iodide (1.2 eq), Cu₂O (0.2 eq), K₃PO₄ (3.0 eq) and TMEDA (0.2 eq) were dissolved in *o*-dichlorobenzene (3 mL/mmol). The resulting mixture was refluxed (185 °C) under argon atmosphere for 24 h. The reaction mixture was concentrated under reduced pressure and the crude was dissolved in CH₂Cl₂ and filtered with a pad of Celite®. Solvent was then evaporated under reduced pressure and the product was purified with flash chromatography on silica gel.

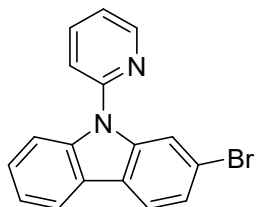
2.2 2,7-dibromo-9-(pyridin-2-yl)-9H-carbazole (1)



The title compound was synthesized using the general procedure for Ullmann coupling reaction using 2,7-dibromo-9H-carbazole (3.00 g, 9.23 mmol, 1.0 eq), 2-iodopyridine (1.18 mL, 11.1 mmol, 1.2 eq), Cu₂O (0.26 g, 1.85 mmol, 0.2 eq), K₃PO₄ (5.88 g, 27.7 mmol, 3.0 eq) and TMEDA (0.28 mL, 1.85 mmol, 0.2 eq) in *o*-dichlorobenzene (30 mL).

After purification with flash chromatography on silica gel [column conditions: silica cartridge (40 g); solid deposit on Celite®; λ_{detection}: (254 nm, 280 nm); gradient petroleum ether/CH₂Cl₂ from 10 % to 50 % in 60 min at 40 mL/min], a colorless powder was obtained (3.62 g, 98 %). ¹H NMR (300 MHz, CD₂Cl₂) δ 8.74 (ddd, *J* = 4.9, 2.0, 0.9 Hz, 1H), 8.03 – 7.94 (m, 5H), 7.61 (ddd, *J* = 8.0, 0.9 Hz, 1H), 7.48 – 7.36 (m, 3H). ¹³C NMR (75 MHz, CD₂Cl₂) δ 150.63, 149.92, 140.51, 138.97, 124.38, 122.50, 122.15, 121.34, 120.01, 119.05, 114.45. HRMS (ASAP, 150 °C): Found [M+H]⁺, 400.928, C₁₇H₁₁N₂Br₂ required 400.928.

2.3 2-bromo-9-(pyridin-2-yl)-9H-carbazole (2)

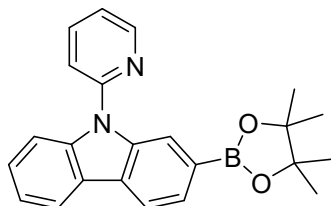


The title compound was synthesized using the general procedure for Ullmann coupling reaction using

2-bromo-9H-carbazole (2.00 g, 8.13 mmol, 1.0 eq), 2-iodopyridine (1.04 mL, 9.75 mmol, 1.2 eq), Cu₂O (0.23 g, 1.63 mmol, 0.2 eq), K₃PO₄ (5.17 g, 24.38 mmol, 3.0 eq) and TMEDA (0.24 mL, 1.63 mmol, 0.2 eq) in *o*-dichlorobenzene (20 mL).

After purification with flash chromatography on silica gel [column conditions: silica cartridge (40 g); solid deposit on Celite®; λ_{detection}: (254 nm, 280 nm); gradient petroleum ether/CH₂Cl₂ from 30 % to 60 % in 60 min at 40 mL/min], the title compound was obtained as a colorless powder (2.61 g, 99 %). ¹H NMR (300 MHz, CD₂Cl₂) δ 8.73 (m, 1H), 8.11 (m, 1H), 8.05 (dd, *J* = 1.7, 0.5 Hz, 1H), 8.02 – 7.93 (m, 2H), 7.79 (dd *J* = 8.3, 0.9 Hz, 1H), 7.63 (dd *J* = 8.1, 0.9 Hz, 1H), 7.52 – 7.42 (m, 2H), 7.35 (m, 2H). ¹³C NMR (75 MHz, CD₂Cl₂) δ 151.15, 149.75, 140.38, 139.68, 138.74, 126.57, 123.90, 123.51, 123.10, 121.73, 121.26, 120.17, 119.55, 119.01, 114.47, 111.21. HRMS (ASAP, 100 °C): Found [M+H]⁺, 323.018 C₁₇H₁₂N₂Br required 323.018.

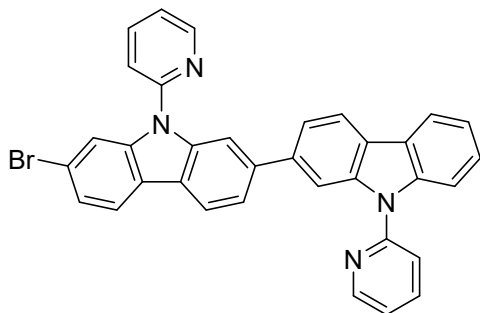
2.4 9-(pyridin-2-yl)-2-(4,4,5,5-tetramethyl-1,3,2-dioxaborolan-2-yl)-9H-carbazole (3)



2-bromo-9-(pyridin-2-yl)-9H-carbazole (2.00 g, 6.19 mmol, 1.0 eq) was dissolved in dry THF (80 mL), *n*-BuLi (2.50 M in hexanes, 2.97 mL, 7.43 mmol, 1.2 eq) was added dropwise at -78 °C under argon atmosphere. The solution was stirred for 1 h min at -78 °C before the addition of 2-isopropoxy-4,4,5,5-tetramethyl-1,3,2-dioxaborolane, (1.70 mL, 8.35 mmol, 1.35 eq). The solution was stirred for an additional time of 15 min at -78°C and the mixture was allowed to warm to room temperature under stirring overnight. The excess of *n*-BuLi was quenched with ethanol and the solvent was removed under reduced pressure. The crude mixture was then dissolved in dichloromethane, washed with water 3 times, dried over Na₂SO₄ and filtered. The residue was purified by flash chromatography on silica gel [column conditions: silica cartridge (40 g); solid deposit on Celite®; λdetection: (254 nm, 280 nm); gradient Petroleum ether/CH₂Cl₂ from 20 % to 60 % in 60 min at 40 mL/min], the title compound was obtained as a colorless powder (1.35 g, 59 %). ¹H NMR (300 MHz, CDCl₃) δ 8.75 (m, 1H), 8.21 (s, 1H), 8.18 – 8.10 (m, 2H), 8.00 – 7.92 (m, 1H), 7.81 (m, 2H), 7.66 (dd *J* = 8.1, 1.0 Hz, 1H), 7.46 (m, 1H), 7.36 – 7.28 (m, 2H), 1.37 (s, 12H). ¹³C NMR (75 MHz, CDCl₃) δ 151.78, 149.77, 140.21, 139.19, 138.59, 127.11, 126.82, 126.79, 124.01, 121.31, 120.84, 120.57, 119.52, 117.07, 111.24, 83.79, 24.91.

Consistent with previous data.⁸

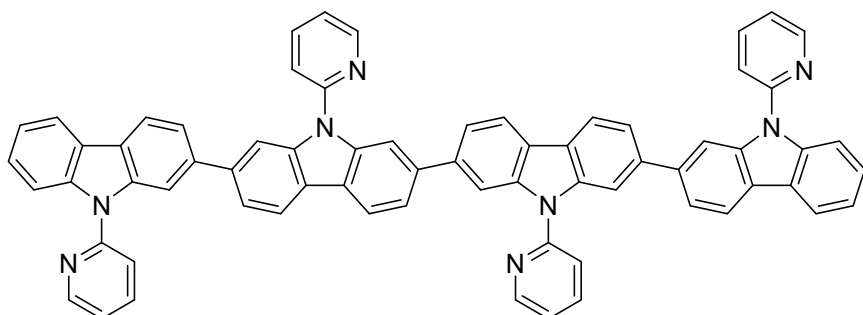
2.5 7-bromo-9,9'-di(pyridin-2-yl)-9H,9'H-2,2'-bicarbazole (4)



2,7-dibromo-9-(pyridin-2-yl)-9H-carbazole (465 mg, 1.16 mmol, 1.0 eq), 9-(pyridin-2-yl)-2-(4,4,5,5-tetramethyl-1,3,2-dioxaborolan-2-yl)-9H-carbazole (428 mg, 1.16 mmol, 1.0 eq), tetrakis(triphenylphosphine)palladium(0) (67 mg, 0.06 mmol, 0.05 eq) and K₂CO₃ (479 mg, 3.47 mmol, 3.0 eq) were dissolved in a solution of degassed THF (10 mL) and degassed H₂O (2 mL) under argon atmosphere. The reaction mixture was under stirring for 17 h at 60 °C. After, the reaction mixture was poured into water and extracted with dichloromethane (3 times). The organic layer was then washed with water (2 times), dried over Na₂SO₄ and filtered. Solvent was then removed under reduced pressure and the crude was purified by flash chromatography on silica gel [column conditions: silica cartridge (24 g); solid deposit on Celite®; λdetection: (254 nm, 280 nm); gradient petroleum ether/CH₂Cl₂ from 20 % to 80 % in 60 min at 30 mL/min], a yellowish powder was obtained (348 mg, 53 %). ¹H NMR (300 MHz, CD₂Cl₂) δ

8.74 (m, 2H), 8.22 – 8.11 (m, 4H), 8.08 – 7.92 (m, 5H), 7.85 (dd J = 8.3, 0.9 Hz, 1H), 7.72 – 7.62 (m, 4H), 7.50 – 7.42 (m, 2H), 7.40 – 7.31 (m, 3H). ^{13}C NMR (75 MHz, CD_2Cl_2) δ 151.65, 151.14, 149.83, 149.68, 140.93, 140.76, 140.29, 140.18, 139.99, 138.83, 138.61, 126.20, 124.06, 123.89, 123.38, 122.92, 122.62, 121.83, 121.45, 121.32, 121.29, 121.01, 120.81, 120.39, 120.32, 120.16, 119.57, 119.20, 119.18, 114.48, 111.24, 110.11, 110.02. HRMS (ASAP, 230 °C): Found [M+H] $^+$ 565.102, $\text{C}_{34}\text{H}_{22}\text{N}_4\text{Br}$ required 565.102.

2.6 9,9',9'',9'''-tetra(pyridin-2-yl)-9H,9'H,9''H,9'''H-2,2':7',2'':7'',2'''-quatercarbazole ([4]L-Py-Cbz)



Bis(1,5-cyclooctadiene)nickel (389 mg, 1.41 mmol, 2.0 eq) was weighed in a glove box. Then, compound **4** (400 mg, 0.71 mmol, 1.0 eq) and bipyridine (221 mg, 1.41 mmol, 2.0 eq) were charged in a round bottom flask under argon flux. Dry THF (12 mL) was added. The resulting mixture was stirred at 70 °C overnight. After cooling to RT, the solution was poured into water and extracted with CH_2Cl_2 (3 times). The organic layer was then washed with water (3 times) dried over Na_2SO_4 , filtered and concentrated under reduced pressure. After purification with flash chromatography on silica gel [column condition: silica cartridge (24 g); solid deposit on Celite®; λ detection: (254 nm, 280 nm); gradient CH_2Cl_2 /light petroleum from 15 to 50 % in 60 min at 35 mL/min], to give the title compound as a yellow powder (150 mg, **88 %**). ^1H NMR (300 MHz, CD_2Cl_2) δ 8.76 (m, 4H), 8.26 – 8.13 (m, 14H), 7.98 (m, 4H), 7.86 (dd, J = 8.3, 0.9 Hz, 2H), 7.79 – 7.65 (m, 10H), 7.46 (ddd, J = 8.4, 7.2, 1.3 Hz, 2H), 7.36 (m, 6H). ^{13}C NMR (75 MHz, CD_2Cl_2) δ 151.67, 149.78, 149.69, 140.78, 140.27, 140.23, 140.18, 138.70, 138.61, 126.15, 123.93, 123.29, 123.10, 121.55, 121.44, 121.01, 120.84, 120.35, 120.13, 119.39, 119.21, 111.26, 110.07. HRMS (MALDI, DCTB): Found [M] $^+$ 970.352, $\text{C}_{68}\text{H}_{42}\text{N}_8$ required 970.353.

3 Photophysical properties

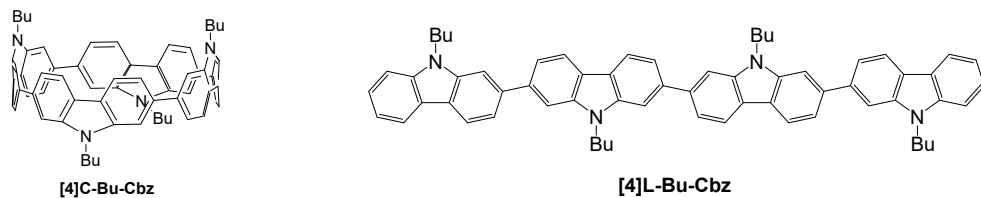


Figure S 1 Molecular structures of [4]C-Bu-Cbz and [4]L-Bu-Cbz.

Table S 1 Physico-chemical properties of [4]C-Py-Cbz and [4]L-Py-Cbz compared to [4]C-Bu-Cbz and [4]L-Bu-Cbz.

	[4]C-Bu-Cbz	[4]L-Bu-Cbz	[4]C-Py-Cbz	[4]L-Py-Cbz
$\lambda_{\text{abs}}^{\text{sol}} [\text{nm}]^{\text{a}}$	337, 292, 256	367, 306, 272	335, 305, 256	361, 301, 258
$\lambda_{\text{abs}}^{\text{film}} [\text{nm}]^{\text{b}}$	345, 294, 268	384, 274	339, 264	379, 310, 260
$\lambda_{\text{em fluo}}^{\text{sol}} [\text{nm}]^{\text{a}} (\lambda_{\text{exc}})$	491 (340)	403, 423 (314)	490 (340)	403, 425 (310)
$\lambda_{\text{em fluo}}^{\text{film}} [\text{nm}] (\lambda_{\text{exc}})^{\text{b}}$	495, 518 (350)	420, 442 (360)	490 (350)	445 (350)
QY ^{sol} ^c	0.20	0.82	0.18	0.57
QY ^{film} ^d	0.13	0.34	0.11	0.32
$\tau_s [\text{ns}] (\lambda_{\text{em}})$	6.2 (483)	<1 (403)	7.1 (490)	<1 (403)
$k_r (\times 10^8) [\text{s}^{-1}]$	0.34	>8.2	0.25	>5.7
$k_{\text{nr}} (\times 10^8) [\text{s}^{-1}]$	1.3	>1.8	1.2	>4.3
$E^{\text{ox}} (\text{V})^{\text{e}}$	0.89, 1.33*, 1.47	0.94*, 1.0, 1.2	1.08, 1.5*, 1.7*, 2.28	0.78, 0.89, 1.22, 1.77
$E^{\text{red}} (\text{V})^{\text{f}}$	-2.23, -2.70	-2.48, -2.71, <-2.95	-2.17, -2.62	-2.34, -2.60, -2.85
HOMO (eV) ^g	-5.18	-5.30	-5.38	-
HOMO (eV) ^h	-5.61	-5.70	-5.56	-5.71
LUMO (eV) ^g	-2.40	-2.17	-2.38	-2.30
HOMO _{theo} (eV) ⁱ	-5.18	-5.31	-5.15	-5.41
LUMO _{theo} (eV) ⁱ	-1.76	-1.66	-1.87	-1.77
$\Delta E_{\text{EL}} (\text{eV})^{\text{j}}$	2.78	3.13	3.00	-
$\Delta E_{\text{theo}} (\text{eV})^{\text{i,j}}$	3.42	3.65	3.28	3.64

a. in cyclohexane for compounds with butyl chain (Bu) and in CH_2Cl_2 for compounds with pyridine (Py), b. in thin solid film prepared from a THF solution (1 mg/mL), c. measured with quinine sulfate in 1 N H_2SO_4 as reference, d. measured with an integrated sphere using [4]cyclo-*N*-butyl-2,7-carbazole [4]C-Bu-Cbz as reference, e. in CH_2Cl_2 f. in DMF g. from electrochemical data h. by Ultraviolet photoelectronic spectroscopy in thin solid film prepared from a CHCl_3 solution i. from TD-DFT B3LYP/6-311+G(d,p) j. $|\text{HOMO-LUMO}|$.

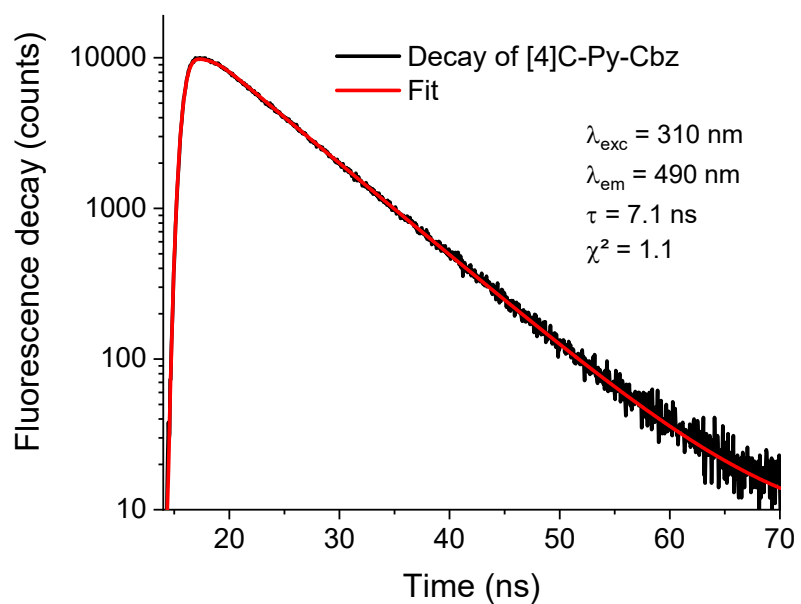


Figure S 2 Fluorescence decay of **[4]C-Py-Cbz** in dichloromethane

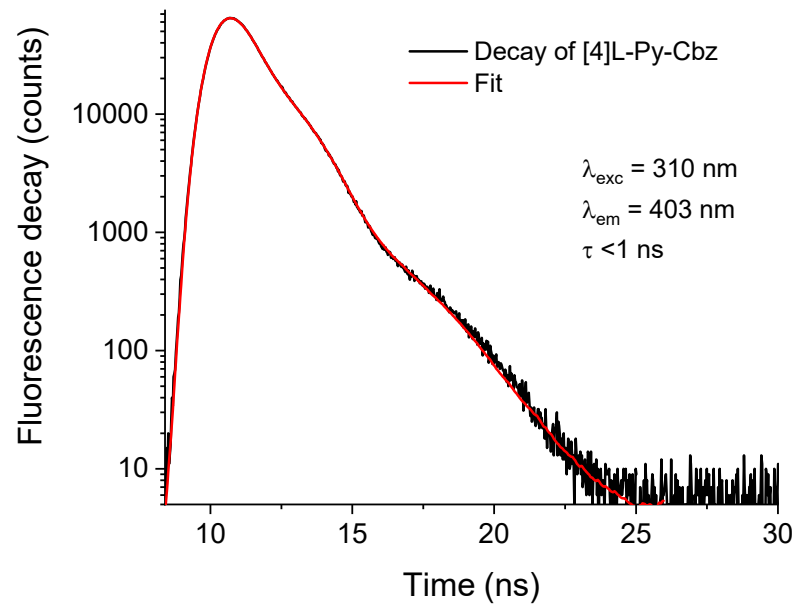


Figure S 3 Fluorescence decay of **[4]L-Py-Cbz** in dichloromethane

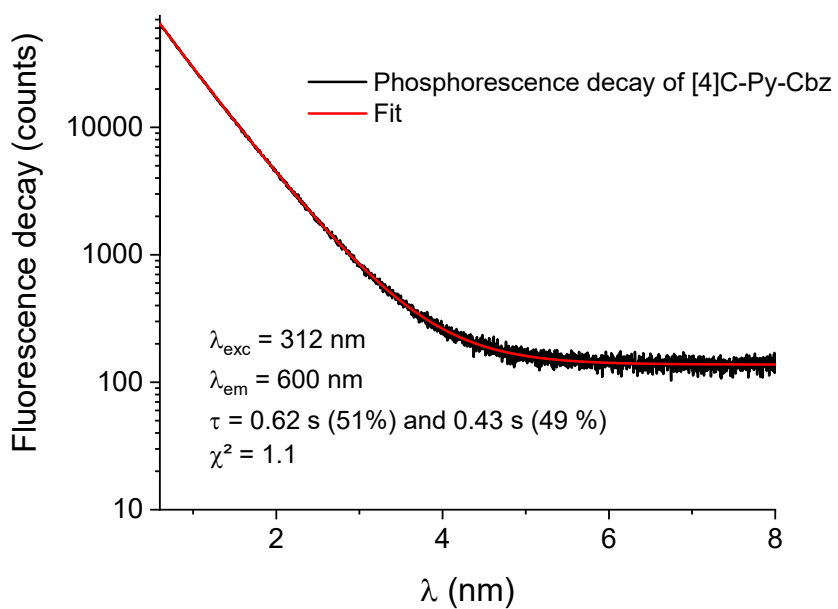


Figure S 4 Phosphorescence decay of $[4]C$ -Py-Cbz in 2-MeTHF

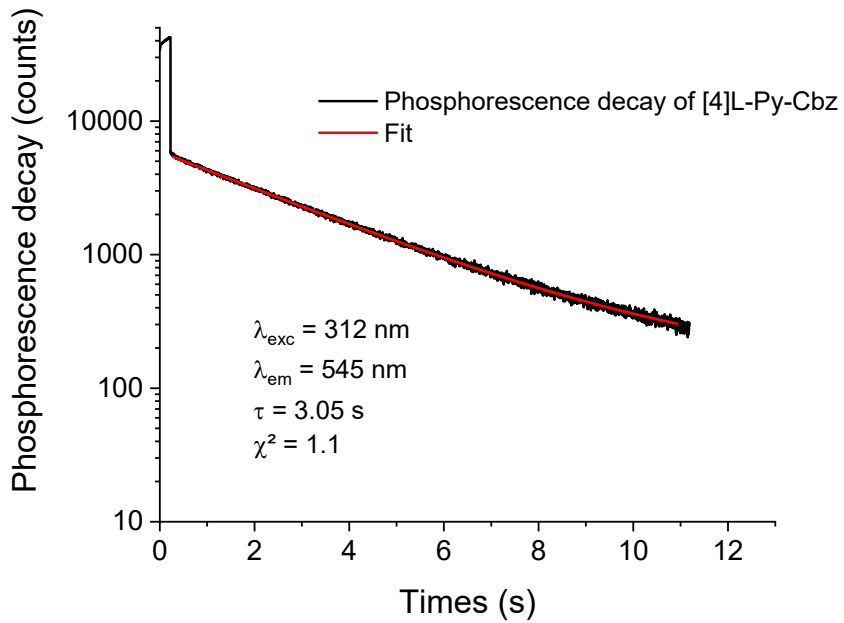


Figure S 5 Phosphorescence decay of $[4]L$ -Py-Cbz in 2-MeTHF

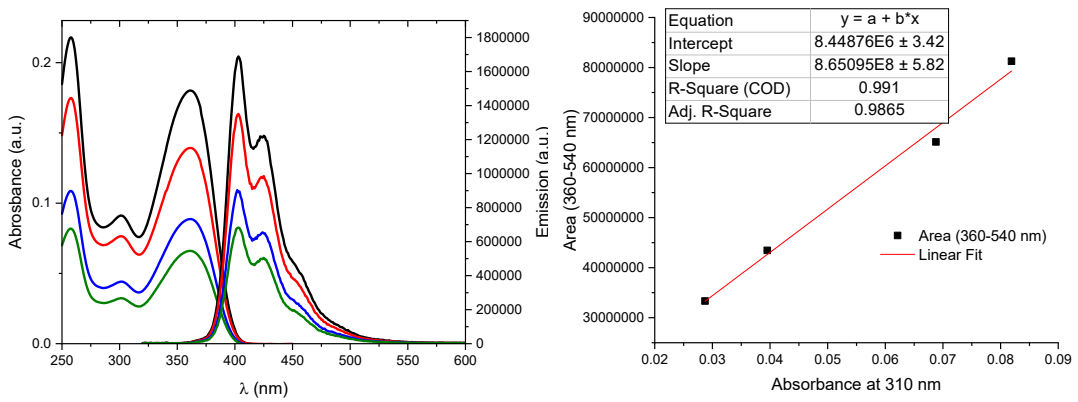


Figure S 6 Absorption and emission spectra of [4]L-Py-Cbz in dichloromethane (left) and linear fit of the integration of the fluorescence between 360 and 540 nm as a function of the absorbance at 310 nm (right).

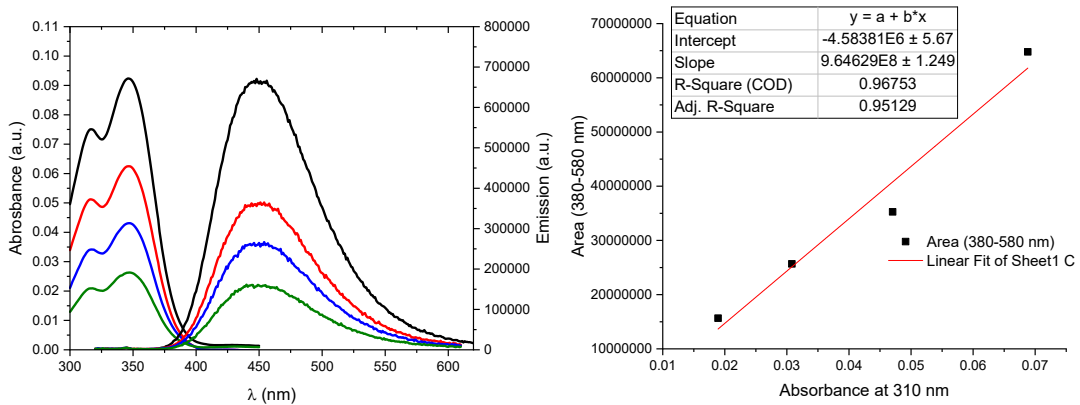


Figure S 7 Absorption and emission spectra of quinine sulfate in 1.0 N sulfuric acid (left) and linear fit of the integration of the fluorescence between 380 and 580 nm as a function of the absorbance at 310 nm (right).

Table S 2 Calculation of the quantum yield of [4]L-Py-Cbz

	Quinine sulfate in 1.0 N H ₂ SO ₄	[4]C-Py-Cbz in dichloromethane
Slope	9.65×10^8	8.65×10^8
Refractive index	1.336	1.421
QY	0.546	0.554

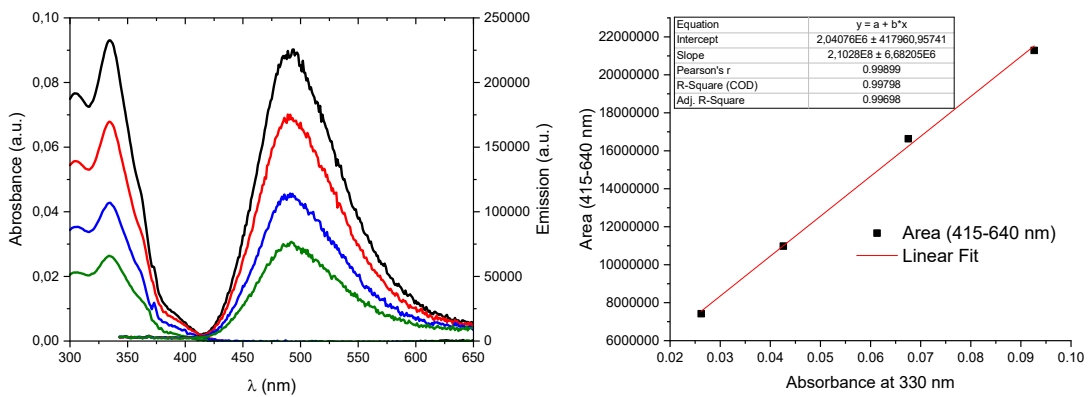


Figure S 8 Absorption and emission spectra of [4]C-Py-Cbz in dichloromethane (left) and linear fit of the integration of the fluorescence between 415 and 640 nm as a function of the absorbance at 330 nm (right).

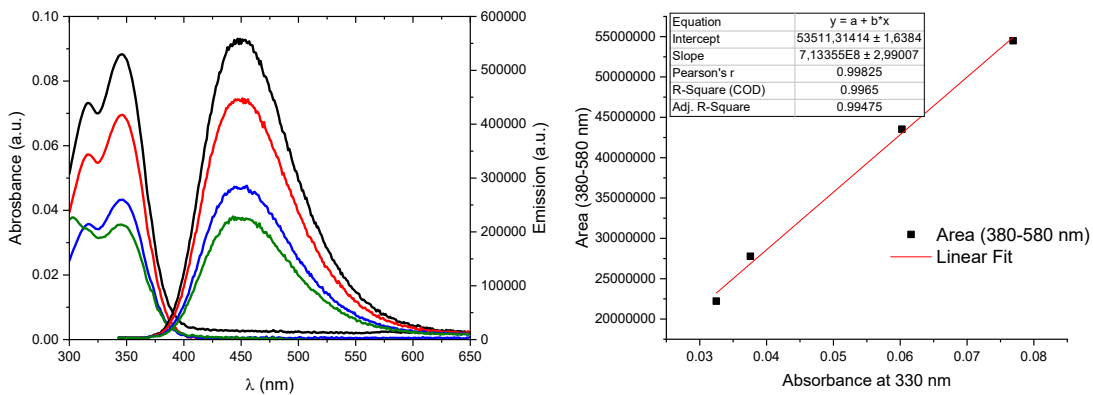


Figure S 9 Absorption and emission spectra of quinine sulfate in 1.0 N sulfuric acid (left) and linear fit of the integration of the fluorescence between 380 and 580 nm as a function of the absorbance at 330 nm (right).

Table S 3 Calculation of the quantum yield of [4]C-Py-Cbz.

	Quinine sulfate in 1.0 N H ₂ SO ₄	[4]C-Py-Cbz in dichloromethane
Slope	7.13×10^8	2.10×10^8
Refractive index	1.336	1.421
QY	0.546	0.182

4 Electrochemical properties

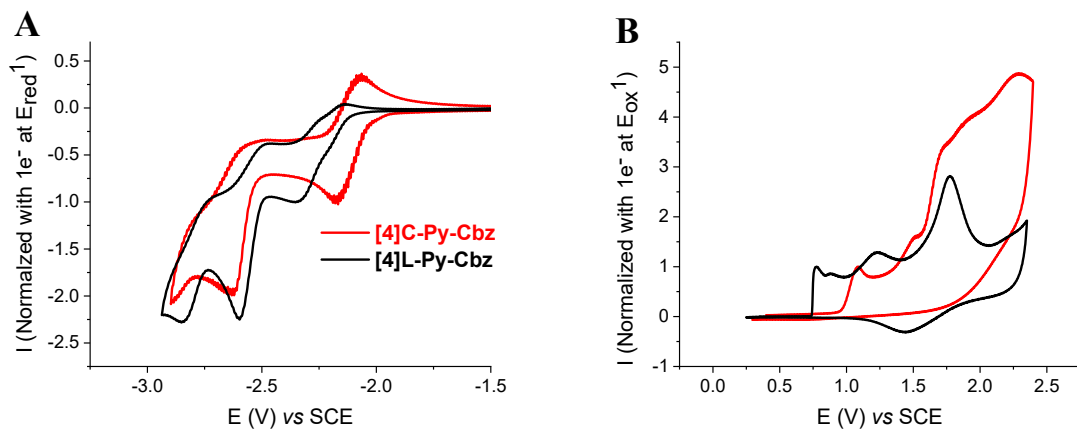


Figure S 10 Normalized CV of [4]C-Py-Cbz (red lines) and [4]L-Py-Cbz (black lines). A. Reduction in $DMF + 0.1\text{ M }Bu_4NPF_6$. B. Oxidation in $DCM + 0.1\text{ M }Bu_4NPF_6$. Scan rate of 100 mV s^{-1} , Platinum disk (diameter of 1 mm) as working electrode.

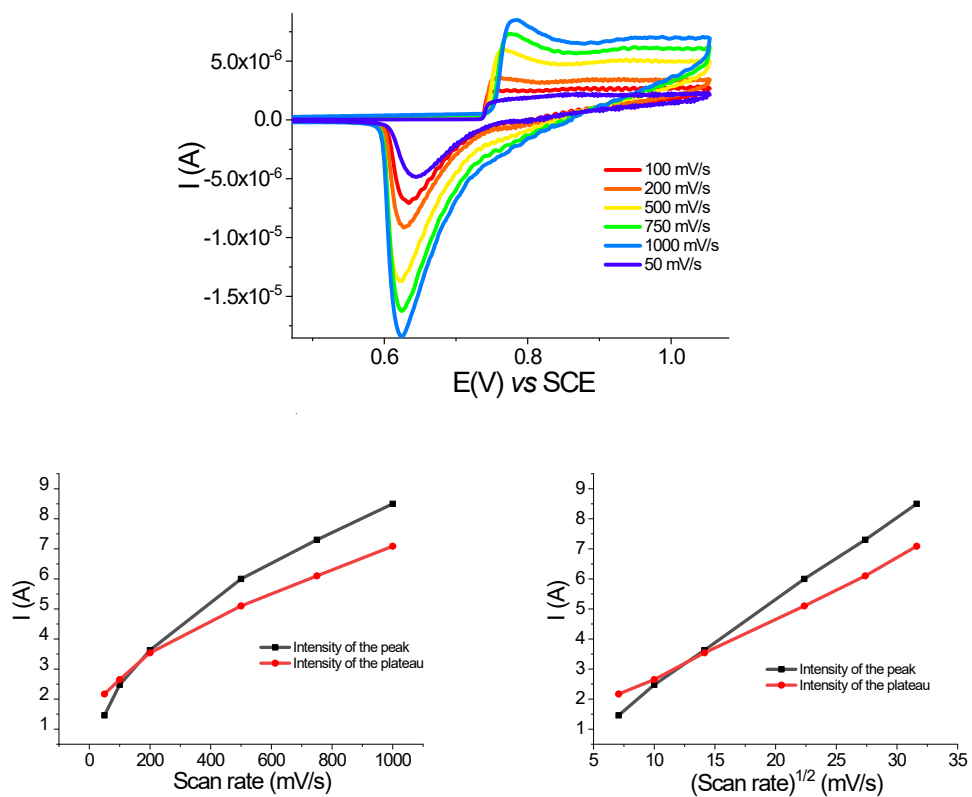


Figure S 11 Top. CV of [4]L-Py-Cbz at different scan rate in dichloromethane. Bottom. Intensity as function of the scan rate (right) and intensity as function of the square root of the scan rate (left)

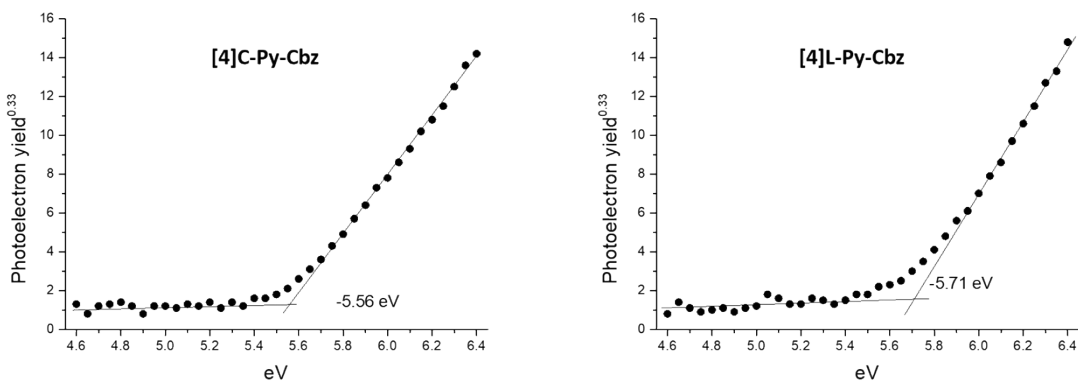


Figure S 12 Determination of HOMO level of [4]C-Py-Cbz (left) and [4]L-Py-Cbz (right) by Ultraviolet photoelectronic spectroscopy (UPS) measurements.

5 Molecular modelling

Table S 4 Results of TD-DFT calculations for [4]C-Py-Cbz

λ (nm)	Oscillator Strength	Major contributions	Minor contributions
447	0.0001	HOMO \rightarrow LUMO (96%)	
372	0.2077	H-1 \rightarrow LUMO (61%), HOMO \rightarrow L+1 (29%)	
371	0.2085	H-2 \rightarrow LUMO (65%), HOMO \rightarrow L+2 (25%)	H-5 \rightarrow LUMO (2%)
367	0.0804	H-1 \rightarrow LUMO (29%), HOMO \rightarrow L+1 (61%)	H-3 \rightarrow LUMO (4%)
365	0.091	H-2 \rightarrow LUMO (26%), HOMO \rightarrow L+2 (69%)	
360	0.0177	H-6 \rightarrow LUMO (18%), H-3 \rightarrow LUMO (67%)	HOMO \rightarrow L+1 (6%)
360	0.1799	H-5 \rightarrow LUMO (16%), H-4 \rightarrow LUMO (72%)	
351	0.0007	HOMO \rightarrow L+3 (82%)	H-6 \rightarrow LUMO (6%), H-3 \rightarrow LUMO (4%), HOMO \rightarrow L+7 (3%)
350	0.0021	HOMO \rightarrow L+4 (85%)	H-5 \rightarrow LUMO (6%), H-4 \rightarrow LUMO (2%)

		H-6→LUMO (42%), H-3→LUMO (16%), HOMO→L+5 (24%)	HOMO→L+3 (6%), HOMO→L+7 (5%)
348	0.154	H-5→LUMO (57%), H-4→LUMO (15%), HOMO→L+8 (12%)	HOMO→L+4 (7%)
347	0.2517	H-6→LUMO (21%), HOMO→L+5 (68%)	H-3→LUMO (3%)
343	0.1755	HOMO→L+6 (72%), HOMO→L+8 (13%)	H-5→LUMO (3%), H-4→LUMO (2%), HOMO→L+10 (3%)
341	0.1209	HOMO→L+7 (70%), HOMO→L+9 (13%)	HOMO→L+3 (6%)
340	0.1235	HOMO→L+6 (20%), HOMO→L+8 (57%)	H-5→LUMO (7%), HOMO→L+4 (2%), HOMO→L+10 (5%)
336	0.148	HOMO→L+7 (14%), HOMO→L+9 (75%)	H-2→L+1 (2%)
334	0.0135	HOMO→L+8 (11%), HOMO→L+10 (79%)	H-1→L+1 (3%)
333	0.0145	H-2→L+2 (54%), H-1→L+1 (19%)	H-2→LUMO (4%), H-1→L+3 (6%)
329	0.113	H-2→L+1 (15%), H-1→L+2 (59%)	H-2→L+3 (5%), H-2→L+5 (2%), H-1→LUMO (4%), HOMO→L+7 (3%)
328	0.0092	H-2→L+2 (27%), H-1→L+1 (57%)	H-3→L+1 (8%), HOMO→L+10 (3%)
324	0.0043		

Table S 5 Results of TD-DFT calculations for [4]L-Py-Cbz

λ (nm)	Oscillator Strength	Major contributions	Minor contributions
385	2.4519	HOMO→LUMO (95%)	
352	0.014	H-3→LUMO (11%), H-2→LUMO (10%), H-1→LUMO (23%),	H-3→L+1 (2%), HOMO→L+2 (9%), HOMO→L+3 (4%),

		HOMO→L+1 (30%)	HOMO→L+4 (2%)
351	0.0148	HOMO→L+2 (44%), HOMO→L+3 (11%), HOMO→L+4 (19%)	H-3→LUMO (9%), H-2→LUMO (4%), H-1→LUMO (6%)
349	0.0529	H-3→LUMO (41%), H-2→LUMO (34%)	H-5→LUMO (3%), H-2→L+1 (3%), H-1→LUMO (3%), H-1→L+1 (4%)
346	0.0235	H-2→LUMO (11%), HOMO→L+1 (47%)	H-5→LUMO (4%), H-5→L+1 (2%), H-4→LUMO (4%), H-3→LUMO (9%), H-1→L+2 (2%), HOMO→L+2 (8%), HOMO→L+5 (5%)
343	0.042	H-5→LUMO (10%), HOMO→L+4 (10%), HOMO→L+5 (55%)	H-5→L+1 (4%), H-4→LUMO (7%)
342	0.0361	H-5→LUMO (26%), HOMO→L+3 (20%), HOMO→L+5 (15%)	H-4→LUMO (3%), H-4→L+1 (6%), H-3→LUMO (3%), HOMO→L+1 (8%), HOMO→L+2 (3%)
341	0.014	H-4→LUMO (19%), HOMO→L+2 (18%), HOMO→L+3 (24%)	H-5→LUMO (2%), H-5→L+1 (6%), HOMO→L+4 (6%), HOMO→L+5 (6%)
339	0.0436	H-5→LUMO (21%), H-4→LUMO (19%), H-4→L+1 (13%), HOMO→L+4 (19%)	H-5→L+1 (3%), HOMO→L+1 (3%), HOMO→L+2 (7%), HOMO→L+5 (3%)
338	0.01	HOMO→L+3 (26%), HOMO→L+4 (27%)	H-5→LUMO (3%), H-5→L+1 (2%), H-4→LUMO (7%), H-4→L+1 (3%)

			H-3→LUMO (2%), H-2→LUMO (4%), H-1→LUMO (4%), H-1→L+3 (3%), HOMO→L+5 (8%)
335	0.0047	H-2→LUMO (17%), H-1→LUMO (45%)	H-4→LUMO (7%), H-3→LUMO (6%), H-3→L+4 (3%), HOMO→L+1 (6%), HOMO→L+4 (4%)
331	0.0159	H-5→L+2 (12%), H-3→L+2 (18%), H-3→L+3 (11%), H-3→L+4 (24%)	H-4→L+2 (3%), H-4→L+3 (5%), H-2→LUMO (2%), H-1→LUMO (5%), H-1→L+2 (4%), H-1→L+3 (2%), H-1→L+4 (3%)
330	0.0462	H-5→L+2 (22%), H-5→L+4 (18%), H-4→L+2 (11%), H-4→L+4 (10%), H-3→L+2 (21%)	H-5→L+1 (4%), H-4→L+1 (2%)
329	0.0321	H-5→L+3 (22%), H-4→L+3 (43%)	H-5→L+4 (3%), H-4→L+1 (3%), H-4→L+2 (5%), H-4→L+4 (4%), H-1→LUMO (3%), HOMO→L+6 (2%)
329	0.0086	HOMO→L+6 (45%), HOMO→L+8 (40%)	
326	0.0432	H-2→L+5 (55%), H-1→L+5 (25%)	H-3→L+5 (2%)
323	0.0037	HOMO→L+9 (80%)	H-2→L+1 (2%), H-2→L+5 (2%), H-1→L+9 (3%),

			HOMO→L+7 (4%)
320	0.0005	HOMO→L+6 (36%), HOMO→L+8 (44%)	H-1→L+6 (5%), H-1→L+8 (4%)
320	0.0002	H-1→L+7 (10%), HOMO→L+7 (75%)	H-2→L+7 (2%), HOMO→L+9 (4%)
316	0.0948	H-2→L+1 (25%), H-1→L+1 (47%)	H-2→LUMO (6%), H-2→L+2 (2%), H-2→L+5 (3%), HOMO→L+9 (5%)

Table S 6 Atomic coordinates of [4]C-Py-Cbz of optimized geometry of S_0 (DFT B3LYP/6-31g(d)) used for TD-DFT.

C	-1.155188	-4.83956	-0.991292
C	2.403309	-4.386093	-1.101349
C	5.576417	-1.698042	-1.318947
C	1.192242	4.956541	-0.753218
C	-2.362908	4.425993	-1.024459
C	-5.523554	1.757472	-1.471174
C	-5.561641	-1.60685	-1.543236
C	-2.431278	-4.316832	-1.199602
C	1.116682	-4.90546	-0.950801
C	5.044149	-2.974963	-1.170715
C	2.468262	4.417665	-0.92492
C	-5.445751	-0.671825	-0.503051
C	-3.34641	-4.32209	-0.134918
C	0.673822	-5.432754	0.284559
C	4.339546	-3.344516	-0.000126
C	3.33657	4.349562	0.174704
C	-5.412263	0.779902	-0.472015
C	-0.777655	-5.398495	0.255416
C	3.276139	-4.390824	-0.003455
C	5.422382	-0.75902	-0.287512
C	0.756567	5.432636	0.504788
C	-3.274353	4.387208	0.042962

C	-4.456788	-2.399694	0.92537
C	-1.757027	-5.562661	1.245422
C	2.896071	-5.090501	1.166725
C	4.889565	-1.194178	0.948221
C	4.355646	2.3623	1.198531
C	1.693898	5.53406	1.544385
C	-2.944332	5.032858	1.257014
C	-4.911304	1.157494	0.798658
C	-4.976268	-1.115515	0.754558
C	-3.025681	-5.026825	1.048607
C	1.610935	-5.602567	1.315271
C	4.350002	-2.472536	1.098436
C	4.858986	1.078491	0.989651
C	2.967905	5.001535	1.375486
C	-1.670831	5.548371	1.474004
C	-4.39022	2.430813	1.027477
C	-1.081455	4.926916	-0.796044
C	-0.695472	5.421736	0.474484
C	-4.987764	3.022541	-1.253826
C	-4.336827	3.341788	-0.039746
C	-5.048744	-2.88897	-1.375171
C	-4.40244	-3.268387	-0.174668
C	5.07288	2.946424	-1.050116
C	4.373922	3.277477	0.133987
C	5.588854	1.669717	-1.24777
C	5.410718	0.692793	-0.25777
N	0.003636	-4.681868	-1.786257
N	-4.794168	-0.002173	1.601635
N	4.684325	-0.078115	1.784449
N	0.07575	4.79196	-1.599679
C	-4.579347	-0.063531	2.988146
C	0.065424	-4.386067	-3.159445
C	0.133037	4.576714	-2.986316
C	4.390237	-0.135754	3.158116
N	-0.89463	3.93508	-3.553953

C	-0.861192	3.733706	-4.876061
C	0.186561	4.136877	-5.698242
C	1.24792	4.822259	-5.101292
C	1.225769	5.059938	-3.733874
N	-0.94177	-3.679437	-3.683485
C	-0.903279	-3.399593	-4.991239
C	0.130934	-3.785723	-5.838547
C	1.170349	-4.539288	-5.287404
C	1.14133	-4.858425	-3.936486
N	-3.922621	0.954205	3.556304
C	-3.721597	0.916956	4.878395
C	-4.140041	-0.12526	5.699938
C	-4.841017	-1.176087	5.102404
C	-5.078498	-1.149581	3.735058
N	3.702893	0.883615	3.684333
C	3.425484	0.849571	4.992714
C	3.795282	-0.191605	5.838766
C	4.528974	-1.243965	5.285393
C	4.845284	-1.22017	3.933712
H	2.65425	-3.802491	-1.979489
H	6.023611	-1.405555	-2.265424
H	-2.567038	3.899351	-1.944523
H	-5.942887	1.505377	-2.44182
H	-5.958958	-1.306523	-2.509309
H	-2.627478	-3.74428	-2.093623
H	5.088572	-3.671076	-2.003885
H	2.709272	3.870483	-1.828977
H	-3.913072	-2.649452	1.829164
H	-1.505738	-6.0279	2.195118
H	3.591893	-5.146844	1.999421
H	3.786902	2.56695	2.093078
H	1.40042	5.936239	2.510553
H	-3.669261	5.043493	2.066245
H	-3.755441	-5.075231	1.852416
H	1.312045	-6.045968	2.261527

H	3.76323	-2.714765	1.976893
H	3.659718	4.99745	2.213106
H	-1.411797	5.963545	2.444605
H	-3.860472	2.626382	1.947601
H	-4.986782	3.747792	-2.062838
H	-5.055085	-3.580136	-2.213316
H	5.132091	3.675714	-1.853625
H	6.049166	1.411475	-2.197993
H	-1.722855	3.214301	-5.292338
H	0.165627	3.934674	-6.764191
H	2.078961	5.187193	-5.698992
H	2.013954	5.626727	-3.253342
H	-1.747891	-2.828567	-5.373034
H	0.115983	-3.518483	-6.89014
H	1.988916	-4.893209	-5.908369
H	1.911409	-5.47763	-3.492417
H	-3.189499	1.770607	5.295142
H	-3.937423	-0.107992	6.765875
H	-5.218029	-2.002044	5.699651
H	-5.656852	-1.929024	3.254026
H	2.870435	1.704039	5.376147
H	3.53094	-0.172311	6.891019
H	4.869881	-2.06891	5.905198
H	5.449818	-2.000928	3.488124

Number of imaginary frequencies: 0

Table S 7 Atomic coordinates of [4]L-Py-Cbz of optimized geometry of S₀ (DFT B3LYP/6-31g(d)) used for TD-DFT.

C	13.124671	0.495944	0.704336
C	14.375643	-0.032603	1.03259
H	14.536602	-1.101937	1.065751
C	15.395516	0.864069	1.346072
H	16.375132	0.474151	1.609255
C	15.184274	2.25286	1.338754
H	16.000538	2.922865	1.593655

C	13.936433	2.773425	1.012048
H	13.76931	3.847325	1.003832
C	12.896646	1.89371	0.689553
C	11.517007	2.096437	0.304879
C	10.717538	3.233304	0.150144
H	11.132943	4.223436	0.318009
C	9.380457	3.087229	-0.197417
H	8.752229	3.96753	-0.29123
C	8.802784	1.810198	-0.379534
C	9.601311	0.665699	-0.231795
H	9.162694	-0.314264	-0.37688
C	10.951205	0.81646	0.088252
C	11.803997	-1.545806	0.089673
C	11.079661	-2.025651	-1.015594
H	10.651879	-1.336479	-1.73388
C	10.962145	-3.400953	-1.181267
H	10.409878	-3.79947	-2.028095
C	11.583271	-4.255336	-0.268188
H	11.520077	-5.334473	-0.364802
C	12.311769	-3.675993	0.768449
H	12.834417	-4.298898	1.49244
C	5.241674	0.552937	-0.468511
C	6.591711	0.660342	-0.1308
H	7.040792	0.008189	0.609008
C	7.3621	1.677623	-0.715823
C	6.754497	2.575509	-1.622421
H	7.363136	3.340985	-2.09387
C	5.404603	2.48269	-1.936881
H	4.954551	3.190402	-2.628071
C	4.630497	1.472754	-1.356537
C	3.228025	1.13236	-1.423014
C	2.142671	1.660962	-2.130841
H	2.282502	2.502063	-2.80486
C	0.887515	1.08856	-1.97779
H	0.049024	1.477526	-2.547128

C	0.680879	-0.016048	-1.118304
C	1.763456	-0.549334	-0.402586
H	1.615716	-1.356715	0.301461
C	3.022806	0.027439	-0.562527
C	4.483714	-1.445356	0.850788
C	5.634124	-2.238704	0.701752
H	6.343417	-2.03511	-0.091429
C	5.818375	-3.305392	1.574119
H	6.700853	-3.932986	1.484175
C	4.849696	-3.570877	2.54353
H	4.954542	-4.394867	3.241921
C	3.72512	-2.749191	2.577278
H	2.929942	-2.928703	3.298798
C	-3.064895	-0.361523	-0.839811
C	-1.8063	0.222061	-0.973465
H	-1.705877	1.293763	-1.077473
C	-0.673963	-0.606121	-0.96743
C	-0.833643	-2.004722	-0.826339
H	0.045702	-2.64061	-0.855923
C	-2.089201	-2.580772	-0.690377
H	-2.189658	-3.658334	-0.590233
C	-3.222994	-1.760453	-0.692596
C	-4.638475	-2.020465	-0.563736
C	-5.397907	-3.188113	-0.437779
H	-4.909429	-4.157048	-0.377565
C	-6.783225	-3.101028	-0.388842
H	-7.369545	-4.004757	-0.256794
C	-7.449323	-1.857367	-0.484646
C	-6.691645	-0.681484	-0.605631
H	-7.193554	0.270168	-0.735243
C	-5.29923	-0.768541	-0.619017
C	-4.582446	1.633827	-0.745039
C	-5.533027	2.173534	0.138811
H	-6.059005	1.533342	0.837101
C	-5.746813	3.546863	0.119578

H	-6.470573	3.991488	0.797753
C	-5.002357	4.343267	-0.752576
H	-5.135793	5.419409	-0.795678
C	-4.058349	3.711657	-1.559344
H	-3.436498	4.291125	-2.239505
C	-10.984523	-0.686676	0.159766
C	-9.589395	-0.721082	0.15757
H	-9.010296	0.039659	0.667695
C	-8.93289	-1.795472	-0.463321
C	-9.70094	-2.82037	-1.062758
H	-9.191726	-3.630024	-1.575651
C	-11.089283	-2.801461	-1.027825
H	-11.657632	-3.608865	-1.4819
C	-11.748084	-1.736397	-0.405799
C	-13.140207	-1.43745	-0.151027
C	-14.332582	-2.092952	-0.47904
H	-14.310774	-3.026706	-1.034813
C	-15.542468	-1.529733	-0.086789
H	-16.476236	-2.027823	-0.332031
C	-15.565255	-0.321718	0.629818
H	-16.519069	0.101155	0.933714
C	-14.391851	0.347978	0.972211
H	-14.413845	1.263974	1.547494
C	-13.17976	-0.221877	0.574842
C	-11.496976	1.49103	1.298284
C	-10.483263	2.266552	0.708855
H	-9.996464	1.934579	-0.200439
C	-10.154661	3.481462	1.298787
H	-9.379462	4.104071	0.859628
C	-10.849593	3.9012	2.434657
H	-10.62587	4.843986	2.923383
C	-11.863109	3.074776	2.915003
H	-12.44989	3.367658	3.783957
N	11.93968	-0.159627	0.310615
N	4.261148	-0.337256	0.006419

N	-4.33627	0.245658	-0.769712
N	-11.860162	0.246742	0.743601
N	12.417939	-2.356009	0.959295
N	3.540957	-1.703383	1.76366
N	-3.851222	2.389893	-1.57143
N	-12.181731	1.892988	2.37472

Number of imaginary frequencies: 0

Table S 8 Atomic coordinates of [4]C-Py-Cbz of optimized geometry of S₀ (DFT B3LYP/6-31+g(d)) used for angles and bond length calculation.

C	-1.155188	-4.83956	-0.991292
C	2.403309	-4.386093	-1.101349
C	5.576417	-1.698042	-1.318947
C	1.192242	4.956541	-0.753218
C	-2.362908	4.425993	-1.024459
C	-5.523554	1.757472	-1.471174
C	-5.561641	-1.60685	-1.543236
C	-2.431278	-4.316832	-1.199602
C	1.116682	-4.90546	-0.950801
C	5.044149	-2.974963	-1.170715
C	2.468262	4.417665	-0.92492
C	-5.445751	-0.671825	-0.503051
C	-3.34641	-4.32209	-0.134918
C	0.673822	-5.432754	0.284559
C	4.339546	-3.344516	-0.000126
C	3.33657	4.349562	0.174704
C	-5.412263	0.779902	-0.472015
C	-0.777655	-5.398495	0.255416
C	3.276139	-4.390824	-0.003455
C	5.422382	-0.75902	-0.287512
C	0.756567	5.432636	0.504788
C	-3.274353	4.387208	0.042962
C	-4.456788	-2.399694	0.92537
C	-1.757027	-5.562661	1.245422
C	2.896071	-5.090501	1.166725

C	4.889565	-1.194178	0.948221
C	4.355646	2.3623	1.198531
C	1.693898	5.53406	1.544385
C	-2.944332	5.032858	1.257014
C	-4.911304	1.157494	0.798658
C	-4.976268	-1.115515	0.754558
C	-3.025681	-5.026825	1.048607
C	1.610935	-5.602567	1.315271
C	4.350002	-2.472536	1.098436
C	4.858986	1.078491	0.989651
C	2.967905	5.001535	1.375486
C	-1.670831	5.548371	1.474004
C	-4.39022	2.430813	1.027477
C	-1.081455	4.926916	-0.796044
C	-0.695472	5.421736	0.474484
C	-4.987764	3.022541	-1.253826
C	-4.336827	3.341788	-0.039746
C	-5.048744	-2.88897	-1.375171
C	-4.40244	-3.268387	-0.174668
C	5.07288	2.946424	-1.050116
C	4.373922	3.277477	0.133987
C	5.588854	1.669717	-1.24777
C	5.410718	0.692793	-0.25777
N	0.003636	-4.681868	-1.786257
N	-4.794168	-0.002173	1.601635
N	4.684325	-0.078115	1.784449
N	0.07575	4.79196	-1.599679
C	-4.579347	-0.063531	2.988146
C	0.065424	-4.386067	-3.159445
C	0.133037	4.576714	-2.986316
C	4.390237	-0.135754	3.158116
N	-0.89463	3.93508	-3.553953
C	-0.861192	3.733706	-4.876061
C	0.186561	4.136877	-5.698242
C	1.24792	4.822259	-5.101292

C	1.225769	5.059938	-3.733874
N	-0.94177	-3.679437	-3.683485
C	-0.903279	-3.399593	-4.991239
C	0.130934	-3.785723	-5.838547
C	1.170349	-4.539288	-5.287404
C	1.14133	-4.858425	-3.936486
N	-3.922621	0.954205	3.556304
C	-3.721597	0.916956	4.878395
C	-4.140041	-0.12526	5.699938
C	-4.841017	-1.176087	5.102404
C	-5.078498	-1.149581	3.735058
N	3.702893	0.883615	3.684333
C	3.425484	0.849571	4.992714
C	3.795282	-0.191605	5.838766
C	4.528974	-1.243965	5.285393
C	4.845284	-1.22017	3.933712
H	2.65425	-3.802491	-1.979489
H	6.023611	-1.405555	-2.265424
H	-2.567038	3.899351	-1.944523
H	-5.942887	1.505377	-2.44182
H	-5.958958	-1.306523	-2.509309
H	-2.627478	-3.74428	-2.093623
H	5.088572	-3.671076	-2.003885
H	2.709272	3.870483	-1.828977
H	-3.913072	-2.649452	1.829164
H	-1.505738	-6.0279	2.195118
H	3.591893	-5.146844	1.999421
H	3.786902	2.56695	2.093078
H	1.40042	5.936239	2.510553
H	-3.669261	5.043493	2.066245
H	-3.755441	-5.075231	1.852416
H	1.312045	-6.045968	2.261527
H	3.76323	-2.714765	1.976893
H	3.659718	4.99745	2.213106
H	-1.411797	5.963545	2.444605

H	-3.860472	2.626382	1.947601
H	-4.986782	3.747792	-2.062838
H	-5.055085	-3.580136	-2.213316
H	5.132091	3.675714	-1.853625
H	6.049166	1.411475	-2.197993
H	-1.722855	3.214301	-5.292338
H	0.165627	3.934674	-6.764191
H	2.078961	5.187193	-5.698992
H	2.013954	5.626727	-3.253342
H	-1.747891	-2.828567	-5.373034
H	0.115983	-3.518483	-6.89014
H	1.988916	-4.893209	-5.908369
H	1.911409	-5.47763	-3.492417
H	-3.189499	1.770607	5.295142
H	-3.937423	-0.107992	6.765875
H	-5.218029	-2.002044	5.699651
H	-5.656852	-1.929024	3.254026
H	2.870435	1.704039	5.376147
H	3.53094	-0.172311	6.891019
H	4.869881	-2.06891	5.905198
H	5.449818	-2.000928	3.488124

Number of imaginary frequencies: 0

Table S 9 Atomic coordinates of [4]L-Py-Cbz of optimized geometry of S_0 (DFT B3LYP/6-31+g(d)) used for angles and bond length calculation.

C	13.129821	0.474515	0.731686
C	14.37843	-0.057684	1.067676
H	14.540811	-1.127684	1.099766
C	15.399825	0.837216	1.38896
H	16.37736	0.445227	1.657937
C	15.18998	2.228178	1.382949
H	16.005903	2.896796	1.643915
C	13.943444	2.751788	1.047663
H	13.779517	3.826525	1.039873
C	12.903243	1.873469	0.717057

C	11.526433	2.077184	0.319491
C	10.726799	3.214396	0.157125
H	11.138373	4.205761	0.329506
C	9.391945	3.067028	-0.206237
H	8.764937	3.948053	-0.307001
C	8.81728	1.788372	-0.3964
C	9.615732	0.644041	-0.240426
H	9.180785	-0.337089	-0.393729
C	10.962391	0.796784	0.097354
C	11.806714	-1.567926	0.121121
C	11.136948	-2.051673	-1.016892
H	10.755019	-1.364533	-1.763595
C	11.012016	-3.428518	-1.175665
H	10.502543	-3.830645	-2.047681
C	11.571715	-4.280052	-0.218931
H	11.501626	-5.359961	-0.307722
C	12.246751	-3.697734	0.853866
H	12.718008	-4.317181	1.614947
C	5.246433	0.551978	-0.493143
C	6.594543	0.659151	-0.14296
H	7.03046	0.024738	0.620849
C	7.379178	1.653694	-0.749439
C	6.788536	2.527142	-1.692408
H	7.406768	3.27605	-2.178935
C	5.44069	2.431033	-2.023503
H	5.005703	3.118828	-2.744413
C	4.651931	1.44405	-1.420888
C	3.247723	1.107687	-1.494077
C	2.172054	1.613841	-2.234595
H	2.321174	2.4311	-2.936007
C	0.91149	1.049214	-2.077469
H	0.08173	1.422301	-2.670638
C	0.691058	-0.027225	-1.184346
C	1.763889	-0.537702	-0.436479
H	1.604168	-1.323544	0.290321

C	3.027215	0.032698	-0.599092
C	4.459029	-1.383019	0.900681
C	5.578172	-2.2231	0.767473
H	6.274868	-2.084642	-0.051578
C	5.748575	-3.249935	1.69119
H	6.606459	-3.91299	1.614594
C	4.795482	-3.42817	2.697402
H	4.889407	-4.217896	3.436543
C	3.701328	-2.563207	2.716926
H	2.92069	-2.672154	3.467672
C	-3.059675	-0.35475	-0.907552
C	-1.79734	0.222813	-1.04597
H	-1.689888	1.294156	-1.156366
C	-0.668005	-0.610588	-1.031706
C	-0.834968	-2.008634	-0.881139
H	0.040801	-2.650534	-0.903984
C	-2.095324	-2.578511	-0.74177
H	-2.199576	-3.655372	-0.634109
C	-3.226063	-1.752053	-0.750201
C	-4.643974	-2.001138	-0.616228
C	-5.412669	-3.163244	-0.483572
H	-4.932695	-4.136592	-0.419241
C	-6.799078	-3.064704	-0.434699
H	-7.392427	-3.964467	-0.302744
C	-7.455708	-1.814621	-0.53151
C	-6.689236	-0.643879	-0.655126
H	-7.184094	0.31302	-0.780728
C	-5.296176	-0.744158	-0.678102
C	-4.563758	1.651512	-0.851552
C	-5.456689	2.225279	0.070303
H	-5.944954	1.609072	0.817212
C	-5.662243	3.600683	0.022886
H	-6.339248	4.073474	0.729964
C	-4.966963	4.363784	-0.919013
H	-5.09489	5.439866	-0.986469

C	-4.080373	3.699521	-1.766551
H	-3.5007	4.250817	-2.504722
C	-10.994693	-0.671889	0.16586
C	-9.597803	-0.702315	0.160177
H	-9.01893	0.034918	0.705645
C	-8.940782	-1.746194	-0.511663
C	-9.708295	-2.740642	-1.163937
H	-9.198263	-3.526224	-1.713231
C	-11.098531	-2.721359	-1.134084
H	-11.665375	-3.503766	-1.632535
C	-11.758432	-1.688761	-0.458344
C	-13.151622	-1.402484	-0.190709
C	-14.346323	-2.034818	-0.559041
H	-14.327213	-2.936789	-1.165736
C	-15.557424	-1.489053	-0.139752
H	-16.49235	-1.969274	-0.415761
C	-15.578892	-0.32009	0.64253
H	-16.532525	0.089426	0.965713
C	-14.402265	0.324823	1.025936
H	-14.426451	1.209329	1.64996
C	-13.190206	-0.227993	0.60126
C	-11.506491	1.425897	1.447865
C	-10.534445	2.270777	0.883742
H	-10.080796	2.025419	-0.07011
C	-10.203638	3.441142	1.559687
H	-9.462196	4.118005	1.142629
C	-10.855418	3.746795	2.757566
H	-10.629248	4.651103	3.314287
C	-11.828033	2.856736	3.212962
H	-12.378227	3.058036	4.130384
N	11.947462	-0.179504	0.330708
N	4.254915	-0.314602	0.000666
N	-4.326207	0.260606	-0.842685
N	-11.871036	0.225957	0.80134
N	12.35892	-2.375397	1.034045

N	3.533274	-1.55599	1.850683
N	-3.882658	2.375173	-1.747396
N	-12.147335	1.717605	2.585495

Number of imaginary frequencies: 0

Table S 10 Atomic coordinates of [4]C-Py-Cbz of optimized geometry of S₁ (TD-DFT B3LYP/6-31+g(d)) used for angles and bond length calculation.

C	2.741897	4.304403	0.817374
C	4.913822	1.45932	1.033619
C	4.960489	-2.669702	1.559249
C	-2.813182	-4.366677	0.716642
C	-4.93355	-1.472924	1.005393
C	-4.978642	2.627728	1.617286
C	-2.601749	4.991599	1.646748
C	1.503058	4.870987	1.074357
C	4.376617	2.716226	0.796163
C	5.501317	-1.419251	1.329612
C	-1.565585	-4.9226	0.962391
C	-3.287638	4.325408	0.601945
C	0.743755	5.386422	-0.011043
C	4.313753	3.271343	-0.515581
C	5.382563	-0.766136	0.061513
C	-0.788622	-5.387972	-0.129393
C	-4.284645	3.306271	0.587827
C	3.29198	4.266918	-0.502188
C	5.392774	0.690986	-0.060757
C	4.26749	-3.331178	0.516042
C	-3.347716	-4.27884	-0.602334
C	-5.412171	-0.689384	-0.07901
C	-1.496596	4.944014	-0.962752
C	2.627749	4.977384	-1.52912
C	5.520935	1.34235	-1.328839
C	4.338338	-2.776941	-0.795668
C	1.435002	-4.89132	-1.074443
C	-2.671124	-4.954392	-1.647182

C	-5.534938	-1.303982	-1.364389
C	-4.34138	2.776446	-0.739814
C	-2.751863	4.405628	-0.717011
C	1.377832	5.514769	-1.284157
C	4.997662	2.60022	-1.558628
C	4.893134	-1.527675	-1.032982
C	2.68161	-4.342139	-0.817236
C	-1.423331	-5.49475	-1.408797
C	-5.014911	-2.557705	-1.61756
C	-4.912452	1.541759	-1.005593
C	-4.379804	-2.715466	0.739538
C	-4.33043	-3.245918	-0.588148
C	-5.516098	1.381358	1.364206
C	-5.401981	0.765044	0.078851
C	-1.346517	5.514444	1.408367
C	-0.713276	5.398613	0.129022
C	1.300489	-5.533551	1.283986
C	0.668425	-5.396196	0.010809
C	2.557738	-5.013664	1.529184
C	3.231947	-4.312418	0.502417
N	3.530313	3.467209	1.645417
N	-3.513997	3.573228	-1.566941
N	3.481788	-3.516	-1.645104
N	-3.563671	-3.523816	1.566628
C	-3.449114	3.567289	-2.971143
C	3.514643	3.395569	3.046989
C	-3.498905	-3.51902	2.970842
C	3.467447	-3.444211	-3.04668
N	-3.784619	-2.371556	3.598415
C	-3.738463	-2.354999	4.937577
C	-3.396939	-3.457414	5.717006
C	-3.118222	-4.657957	5.054109
C	-3.176131	-4.701662	3.666757
N	2.370624	3.709345	3.669859
C	2.344649	3.657637	5.008706

C	3.431685	3.28386	5.794448
C	4.629231	2.976523	5.137525
C	4.683519	3.038276	3.751202
N	-3.750592	2.423776	-3.59855
C	-3.704422	2.406321	-4.9377
C	-3.347516	3.50375	-5.717276
C	-3.052333	4.700448	-5.054558
C	-3.109879	4.745216	-3.667224
N	2.319334	-3.742119	-3.669809
C	2.294419	-3.69018	-5.008668
C	3.386739	-3.331608	-5.794167
C	4.588266	-3.040853	-5.136965
C	4.641341	-3.103228	-3.750625
H	4.762014	0.982477	1.994742
H	4.997664	-3.103635	2.55543
H	-4.795951	-1.038562	1.983582
H	-5.017506	3.046065	2.619707
H	-3.020929	5.017639	2.649374
H	1.053712	4.724673	2.044551
H	5.973969	-0.889821	2.152431
H	-1.099793	-4.791604	1.931794
H	-1.032614	4.806389	-1.932107
H	3.059942	5.033358	-2.525035
H	5.986331	0.80635	-2.151538
H	0.987875	-4.738655	-2.044687
H	-3.090566	-4.974443	-2.649835
H	-5.989262	-0.744345	-2.176679
H	0.841852	5.996092	-2.097863
H	5.041086	3.03355	-2.554818
H	4.748219	-1.048739	-1.994125
H	-0.875824	-5.947125	-2.230237
H	-5.059615	-2.975398	-2.62001
H	-4.780918	1.105458	-1.983752
H	-5.978148	0.82816	2.176548
H	-0.792793	5.959247	2.229771

H	0.757743	-6.007466	2.097556
H	2.988965	-5.075756	2.525155
H	-3.983719	-1.40173	5.402641
H	-3.363676	-3.382634	6.799492
H	-2.876053	-5.557839	5.613706
H	-3.005598	-5.627869	3.130119
H	1.395109	3.926497	5.468751
H	3.348762	3.248266	6.876315
H	5.519185	2.709513	5.70185
H	5.608539	2.845811	3.220136
H	-3.962776	1.456451	-5.402626
H	-3.315084	3.428304	-6.799739
H	-2.797625	5.596782	-5.614282
H	-2.926637	5.66908	-3.130734
H	1.341352	-3.945867	-5.468931
H	3.304594	-3.294972	-6.876058
H	5.481984	-2.786274	-5.701086
H	5.568807	-2.923575	-3.219338

Number of imaginary frequencies: 0

Table S11 Atomic coordinates of [4]L-Py-Cbz of optimized geometry of S₁ (TD-DFT B3LYP/6-31+g(d)) used for angles and bond length calculation.

C	13.19514	0.429576	0.443537
C	14.454525	-0.152387	0.606844
H	14.59407	-1.221693	0.510119
C	15.522057	0.688884	0.928717
H	16.50995	0.256558	1.065126
C	15.344998	2.075719	1.090709
H	16.196789	2.699873	1.347313
C	14.087791	2.650983	0.927948
H	13.949473	3.722213	1.050854
C	12.999343	1.827768	0.599513
C	11.604569	2.091566	0.353524
C	10.817012	3.25365	0.382862
H	11.265121	4.214827	0.621713

C	9.456858	3.166498	0.128305
H	8.85282	4.066139	0.187602
C	8.823009	1.920644	-0.138509
C	9.61653	0.75037	-0.171657
H	9.156107	-0.20582	-0.388867
C	10.98689	0.849417	0.050003
C	11.779094	-1.512299	-0.273171
C	11.005004	-1.850424	-1.397608
H	10.574205	-1.075006	-2.021231
C	10.842023	-3.197118	-1.707877
H	10.254926	-3.487398	-2.575589
C	11.464413	-4.162136	-0.91065
H	11.367626	-5.222986	-1.121099
C	12.238483	-3.718393	0.161581
H	12.760232	-4.428675	0.800544
C	5.277857	0.638414	-0.226558
C	6.647035	0.682016	-0.002925
H	7.155098	-0.132259	0.499559
C	7.37264	1.847054	-0.358724
C	6.668283	2.943305	-0.936961
H	7.225267	3.821072	-1.24891
C	5.302784	2.906575	-1.148527
H	4.794086	3.757752	-1.593316
C	4.57348	1.751856	-0.784268
C	3.19484	1.419213	-0.801226
C	2.031589	2.100944	-1.230749
H	2.109688	3.091281	-1.671642
C	0.801187	1.494751	-1.102984
H	-0.074026	2.018722	-1.469777
C	0.650264	0.178835	-0.54809
C	1.826737	-0.505148	-0.109911
H	1.758822	-1.464118	0.382102
C	3.055468	0.108873	-0.242678
C	4.646068	-1.654057	0.580081
C	5.758304	-2.362799	0.092871

H	6.373036	-1.945861	-0.696668
C	6.026492	-3.620278	0.62444
H	6.880801	-4.189695	0.267644
C	5.174783	-4.145857	1.600488
H	5.348214	-5.122859	2.041027
C	4.075561	-3.378284	1.984116
H	3.369386	-3.750776	2.724072
C	-3.075754	-0.2678	-0.378755
C	-1.849619	0.350805	-0.499905
H	-1.802334	1.42168	-0.630006
C	-0.657219	-0.435548	-0.429458
C	-0.793354	-1.853584	-0.249676
H	0.096537	-2.472652	-0.235651
C	-2.02217	-2.467494	-0.147808
H	-2.087043	-3.546393	-0.034316
C	-3.201425	-1.684361	-0.200162
C	-4.580971	-1.987968	-0.110756
C	-5.313362	-3.192139	0.023407
H	-4.79341	-4.138829	0.143878
C	-6.693014	-3.154461	0.00667
H	-7.237534	-4.081761	0.147168
C	-7.422825	-1.935809	-0.153488
C	-6.687188	-0.723271	-0.266089
H	-7.207615	0.209437	-0.443648
C	-5.302643	-0.757106	-0.223484
C	-4.671806	1.670025	-0.342587
C	-5.660011	2.174074	0.522247
H	-6.179112	1.513481	1.207478
C	-5.921338	3.540092	0.504502
H	-6.672442	3.956622	1.170834
C	-5.188778	4.365658	-0.354679
H	-5.358683	5.437212	-0.397713
C	-4.207847	3.770039	-1.146314
H	-3.595411	4.371519	-1.815841
C	-11.011501	-0.788594	0.049414

C	-9.622392	-0.756914	0.096572
H	-9.105632	0.141539	0.410517
C	-8.886171	-1.934986	-0.193329
C	-9.613442	-3.116085	-0.52771
H	-9.072129	-4.014713	-0.802541
C	-10.9975	-3.146845	-0.546609
H	-11.516902	-4.068007	-0.79855
C	-11.724088	-1.981926	-0.244446
C	-13.126197	-1.688144	-0.1185
C	-14.288147	-2.456876	-0.297372
H	-14.216146	-3.502687	-0.585213
C	-15.530187	-1.858885	-0.104112
H	-16.437904	-2.441498	-0.237266
C	-15.621204	-0.504113	0.266798
H	-16.599667	-0.055895	0.419023
C	-14.480659	0.280676	0.457304
H	-14.558372	1.31444	0.769407
C	-13.236646	-0.322378	0.26078
C	-11.641937	1.588887	0.558693
C	-10.667471	2.236403	-0.221873
H	-10.160151	1.704399	-1.018949
C	-10.403647	3.579211	0.029052
H	-9.661534	4.106188	-0.565408
C	-11.122102	4.241817	1.028733
H	-10.950909	5.290269	1.253587
C	-12.089656	3.5156	1.722891
H	-12.689773	3.990136	2.49732
N	11.967034	-0.160063	0.083525
N	4.344804	-0.365826	0.08805
N	-4.373399	0.291583	-0.359742
N	-11.941771	0.227844	0.341376
N	12.391408	-2.428152	0.486352
N	3.813131	-2.158061	1.498457
N	-3.951076	2.455184	-1.153395
N	-12.345646	2.218897	1.506924

6 Structural properties

6.1 Displacement angle

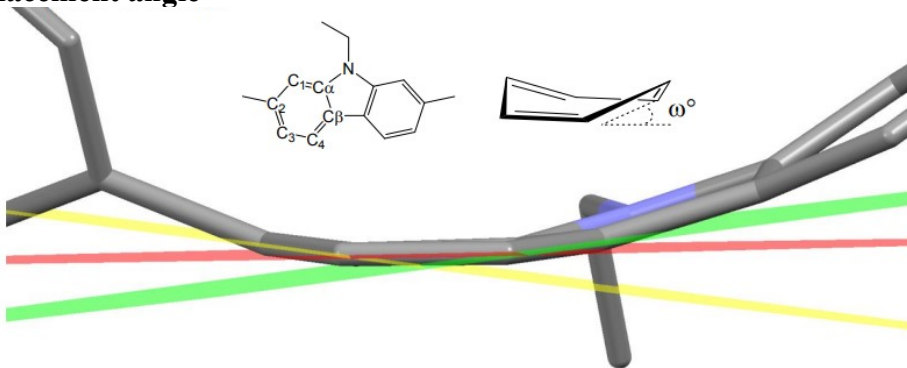


Figure S 13 Measurement of a displacement angle

The displacement angle can represent the deformation of a phenyl unit. Definition of a displacement angle: The mean planes passing by $C\alpha$ -C1-C3-C4 (red), C1-C2- C3 (yellow) and $C\alpha$ -C β -C4 (green) are drawn. The external displacement angle (ω_{ext}) is measured between red and yellow planes, and, the internal displacement angle (ω_{int}) between red and green planes. Then, the mean displacement angle is calculated considering two ω_{ext} and two ω_{int} for each carbazole building units.

Table S 12 Displacement angle values

	ω_{ext} (°)		ω_{int} (°)		ω (°)
	Values	Average	Values	Average	
[4]C-Py-Cbz	9.27	7.23	8.95	6.42	6.83
	7.65		5.96		
	6.33		5.15		
	7.97		6.1		
	7.60		8.02		
	4.11		3.03		
	8.57		8.39		
	6.37		5.76		
[4]L-Py-Cbz	0.81	1.17	0.27	1.08	1.13
	0.81		0.49		
	1.24		0.68		
	1.38		0.36		
	1.16		0.71		
	0.73		1.26		
	2.33		4.00		
	0.93		0.88		

6.2 Torsion angle

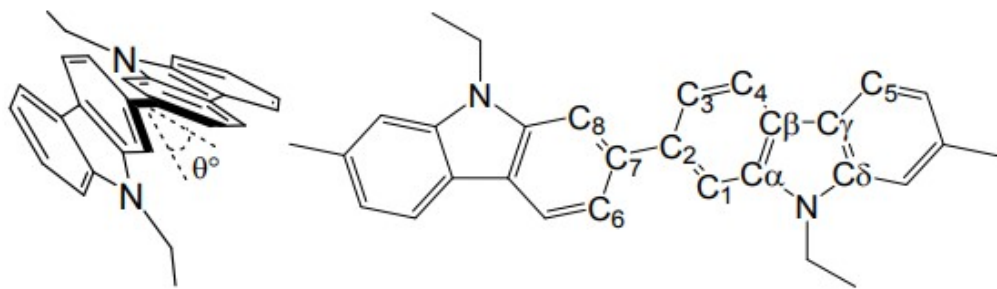


Figure S 14 Definition of the torsion angle between two carbazole units

Definition of a torsion angle: The external torsion angle (θ_{ext}) is the dihedral angle between two carbazole building units. Two angles are measured for each C2-C7 link (C8-C7-C2-C3 and C6-C7-C2-C1). The internal torsion angles (θ_{int}) are the dihedral angles within a building unit (C4-C β -C γ -C5 and C α -C β -C γ -C δ).

Table S 13 Torsion angle values

	$\theta_{\text{ext}} (\circ)$		$\theta_{\text{int}} (\circ)$		$\theta (\circ)$
	Values	Average	Values	Average	
[4]C-Py-Cbz	49.15	46.43	0.95	2.31	24.37
	45.32		3.20		
	50.85		1.62		
	51.30		1.86		
	46.02		1.56		
	49.87		5.76		
	39.08		3.52		
	39.81		0.03		
[4]L-Py-Cbz	16.10	13.09	0.60	3.03	8.06
	15.16		0.92		
	5.57		1.39		
	6.89		3.86		
	17.05		5.55		
	17.75		0.53		
			8.99		
			2.37		

6.3 Dihedral angle between carbazole and substituent

Table S 14 Dihedral angle between carbazole and substituent values from X-Ray structures

	Angle values (°)	γ
[4]C-Py-Cbz	41.98	36.7
	36.03	
	33.3	
	42.12	
	31.41	
	30.95	
	37.71	
	40.08	
[4]L-Py-Cbz	44.45	42.3
	33.68	
	40.67	
	41.05	
	48.1	
	44.65	
	47.96	
	37.92	

6.4 Torsion angle between two carbazoles at S_0 from optimized structures of [4]C-Py-Cbz and [4]L-Py-Cbz (B3LYP/6-31+g(d))

Table S 15 Torsion angle values between two carbazoles at S_0

	Angle values (°)	θ_{ext}
[4]C-Py-Cbz	40.45	40.3
	40.45	
	40.06	
	40.47	
	40.04	
	40.04	
	40.47	
	40.05	
[4]L-Py-Cbz	41.54	39.5
	41.68	
	39.1	
	38.3	
	37.74	
	38.61	

6.5 Torsion angle between two carbazoles at S₁ from optimized structures of [4]C-Py-Cbz and [4]L-Py-Cbz (B3LYP/6-31+g(d))

Table S 16 Torsion angle values between two carbazoles at S₁

	Angle values (°)	θ_{ext}
[4]C-Py-Cbz	28.58	28.4
	28.58	
	27.98	
	29.02	
	28.19	
	28.2	
	29.02	
	27.98	
[4]L-Py-Cbz	29.34	23.0
	30.27	
	18.49	
	17.62	
	21.48	
	20.98	

7 Organic field effect transistor and space-charged-limited current diode measurements

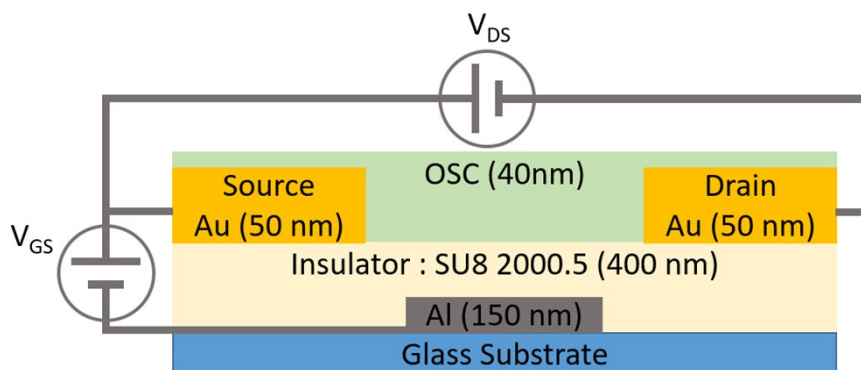


Figure S 15 Structure of the bottom-gate bottom-contact p-type channel OFETs on glass substrate.

OFET: Gate Bias Stress measurement

A gate bias stress is employed herein to estimate the electrical stability of [4]C-Py-Cbz and [4]L-Py-Cbz based OFETs. The threshold voltage shift was evaluated by measuring transfer characteristics (I_D vs. V_{GS}) from $V_{GS}=10$ V to $V_{GS}=-60$ V every 10 minutes. Between two measurements, constant voltages were applied on gate electrode ($V_{GS}=-40$ V) and on drain electrode ($V_{DS} = -10$ V).

The Stretched exponential model has been applied on ΔV_{TH} to evaluate the structural trap effect on the electrical stability of OFETs according to the following relationship.

$$V_{TH}(t) - V_{TH}(t = 0) = \Delta V_{TH} \max \left(1 - e^{-\left(\frac{t}{\tau}\right)^{\beta}} \right) \quad (1)$$

Where $\Delta V_{TH} \max$ is the maximum threshold voltage shift under unlimited stress time, $V_{TH}(t=0)$ is the initial threshold voltage, $V_{TH}(t)$ is threshold voltage at the stress time t . β is related to width of the involved trap distribution and τ is related to trapping time.

Activation energy was extracted from the slope of field effect mobility in neperian logarithmic representation as a function of the inverse of the temperature ($1000/T$) (relation n°2).

$$\mu = \mu_0 \exp \left(-\frac{E_a}{k_B T} \right) \quad (2)$$

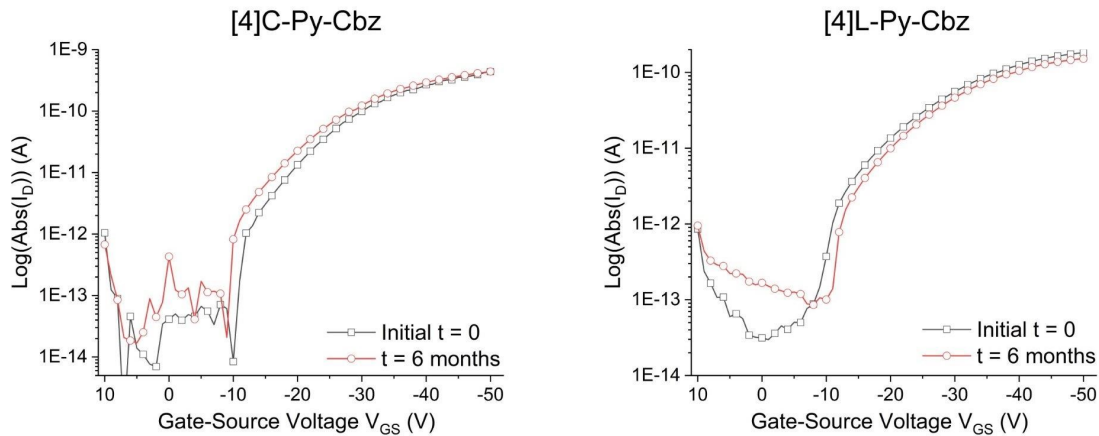


Figure S 16 Transfer characteristics in linear regime of [4]C-Py-Cbz (left) and [4]L-Py-Cbz (right) at $t=0$ s (black lines) and after 6 months (red lines).

8 Atomic Force Microscopy measurement

AFM images were recorded on the Bruker Multimode 8 using PeakForce Tapping with a resolution of 512 x 512 pixels on a 500 nm x 500 nm surface. Scan rate has been set at 1 Hz. Each scan line in the image was scanned from left to right (trace) and from right to left (retrace). The observed topographic features were verified for their consistency between trace and retrace images. Amplitude setpoint was set to 1.68 mV and the drive amplitude was set to 10.38 mV. Roughness has been extracted from these images using Nano Scope Analysis 1.8 after a clean image treatment.

Table S 17 Roughness parameters extracted from AFM images ($500 \times 500 \text{ nm}^2$) of [4]C-Py-Cbz and [4]L-Py-Cbz

	R_a (Arithmetic Average Roughness) [nm]	R_q (RMS Roughness) [nm]	R_{\max} (Maximum Roughness depth) [nm]
[4]C-Py-Cbz	0.76	0.98	8.83
[4]L-Py-Cbz	0.52	0.65	5.89

9 Thermal properties

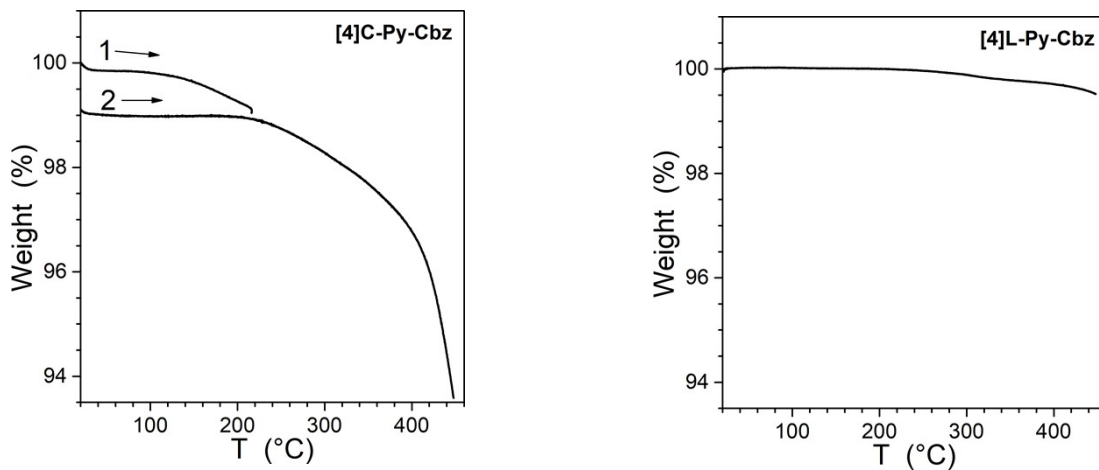


Figure S 17 TGA measurement of [4]C-Py-Cbz and [4]L-Py-Cbz.

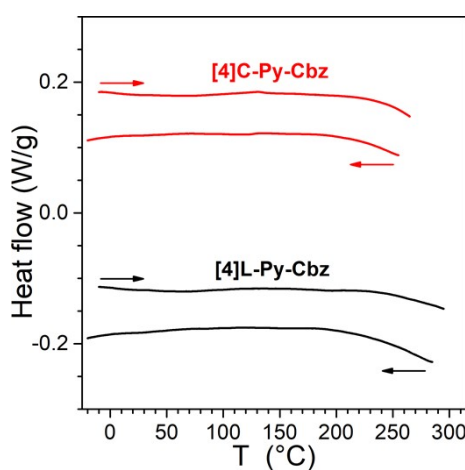
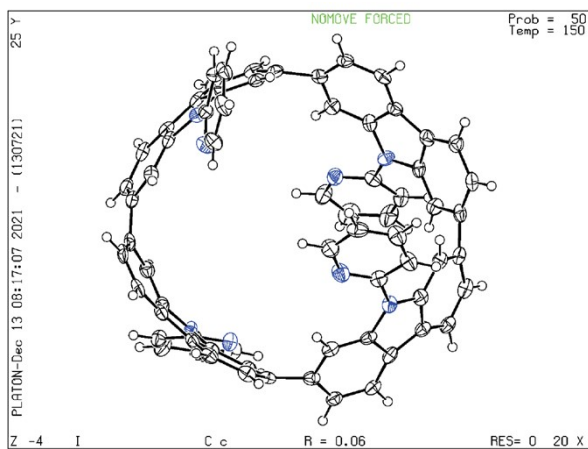


Figure S 18 DSC measurement (2nd heating and 2nd cooling cycle) of [4]C-Py-Cbz (top) and [4]L-Py-Cbz (bottom).

10 X-Ray parameters



[4]C-Py-Cbz

Table S 18 Refinement parameters of [4]C-Py-Cbz.

	[4]C-Py-Cbz
Chemical formula	C ₆₈ H ₄₀ N ₈
M _r	484.54
Crystal system, space group	Monoclinic, Cc
Temperature (K)	150
a, b, c (Å)	13.7773 (13), 24.331 (2), 17.5236 (16)
β (°)	111.036 (4)
V(Å ³)	5482.7 (9)
Z	8
Radiation type	Mo Kα
μ (mm ⁻¹)	0.07
Crystal size (mm)	0.09 × 0.04 × 0.02
Absorption correction	Multi-scan
T _{min} , T _{max}	0.997, 0.999
No. of measured, independent and observed [I > 2σ(I)] reflections	21229, 11588, 9338
R _{int}	0.047
R[F ² > 2σ(F ²)], wR(F ²), S	0.061, 0.152, 1.03
No. of reflections	11588
No. of parameters	688
Δρ _{max} , Δρ _{min} (e Å ⁻³)	0.79, -0.23

[4]L-Py-Cbz

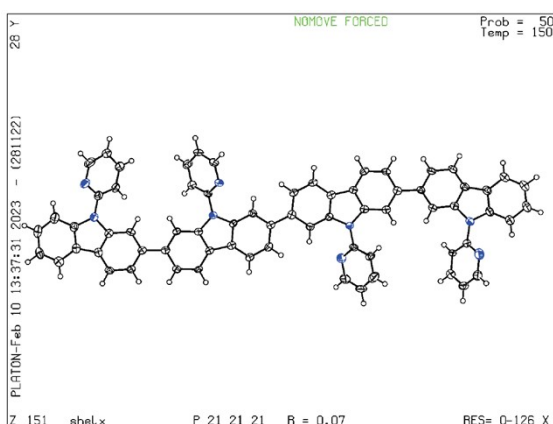


Table S 19 Refinement parameters of [4]L-Py-Cbz.

Empirical formula	C ₆₈ H ₄₂ N ₈
Formula weight	971.09
Temperature	150(2) K
Wavelength	0.71073 Å
Crystal system	Orthorhombic
Space group	P 21 21 21
Unit cell dimensions	a = 7.8187(10) Å α= 90°. b = 13.8355(18) Å β= 90°. c = 43.715(6) Å γ = 90°.
Volume	4728.9(11) Å ³
Z	4
Density (calculated)	1.364 Mg/m ³
Absorption coefficient	0.082 mm ⁻¹
F(000)	2024
Crystal size	0.180 x 0.120 x 0.040 mm ³
Theta range for data collection	2.375 to 27.497°.
Index ranges	-10<=h<=8, -17<=k<=17, -56<=l<=56
Reflections collected	74326
Independent reflections	10792 [R(int) = 0.0873]
Completeness to theta = 25.242°	99.9 %
Refinement method	Full-matrix least-squares on F ₂
Data / restraints / parameters	10792 / 0 / 686
Goodness-of-fit on F ₂	1.092
Final R indices [I>2sigma(I)]	R1 = 0.0744, wR2 = 0.1356
R indices (all data)	R1 = 0.1089, wR2 = 0.1466
Absolute structure parameter	0(4)
Extinction coefficient	n/a
Largest diff. peak and hole	0.220 and -0.279 e.Å ⁻³

11 Copy of NMR Spectra

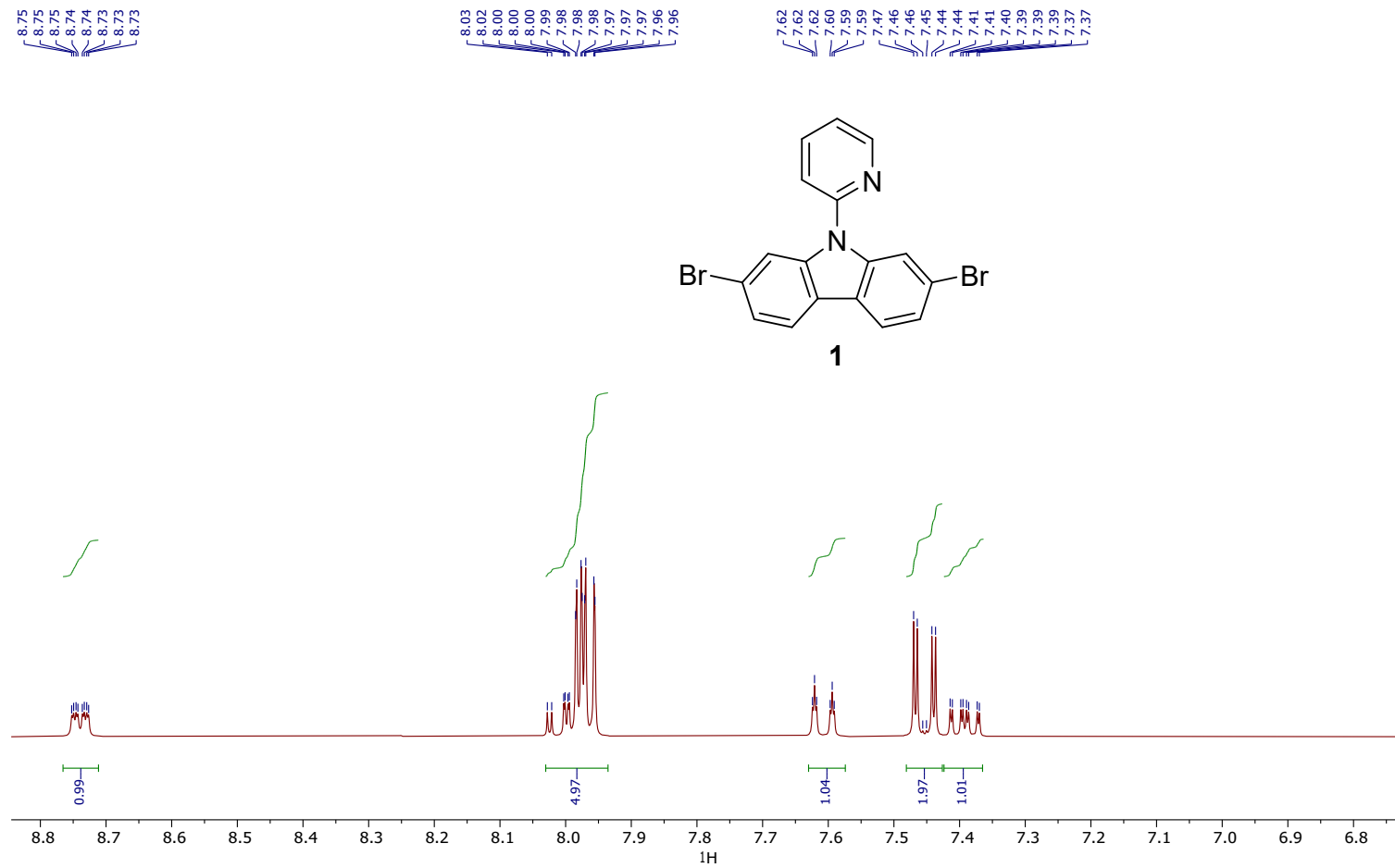


Figure S 19 ^1H -NMR of **1** in CD_2Cl_2

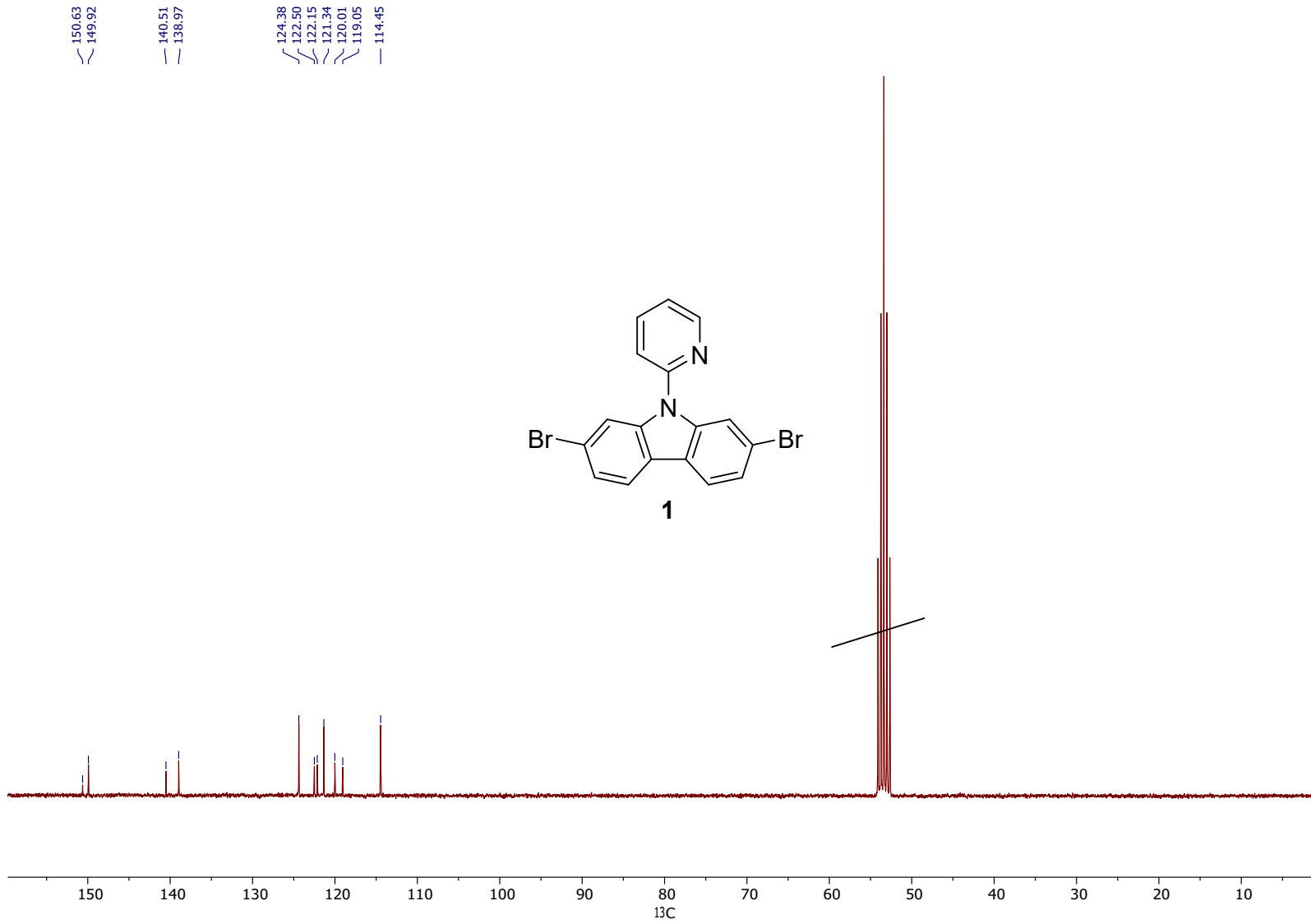


Figure S 20 ^{13}C -NMR of **1** in CD_2Cl_2

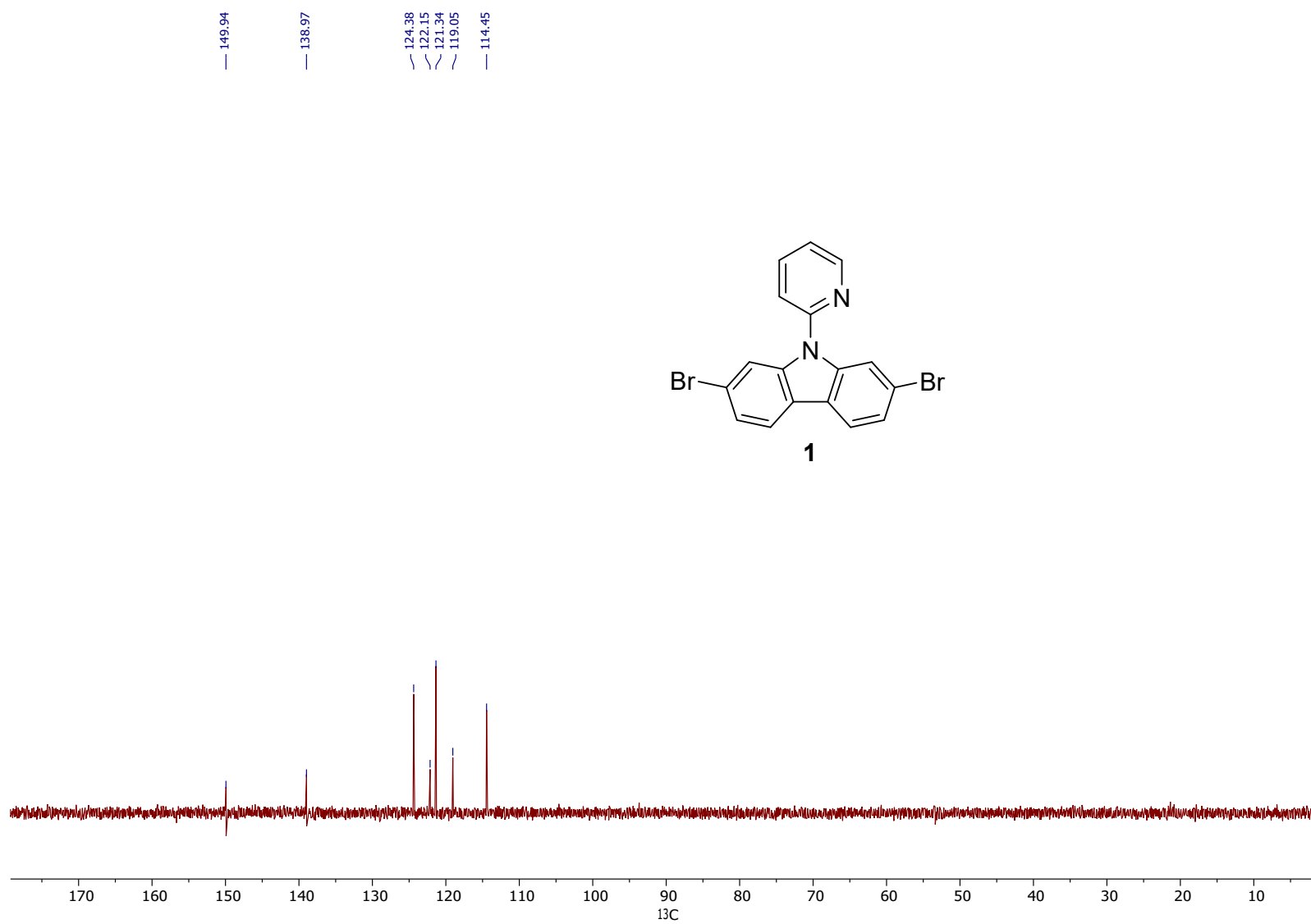


Figure S 21 DEPT-135 of **1** in CD_2Cl_2

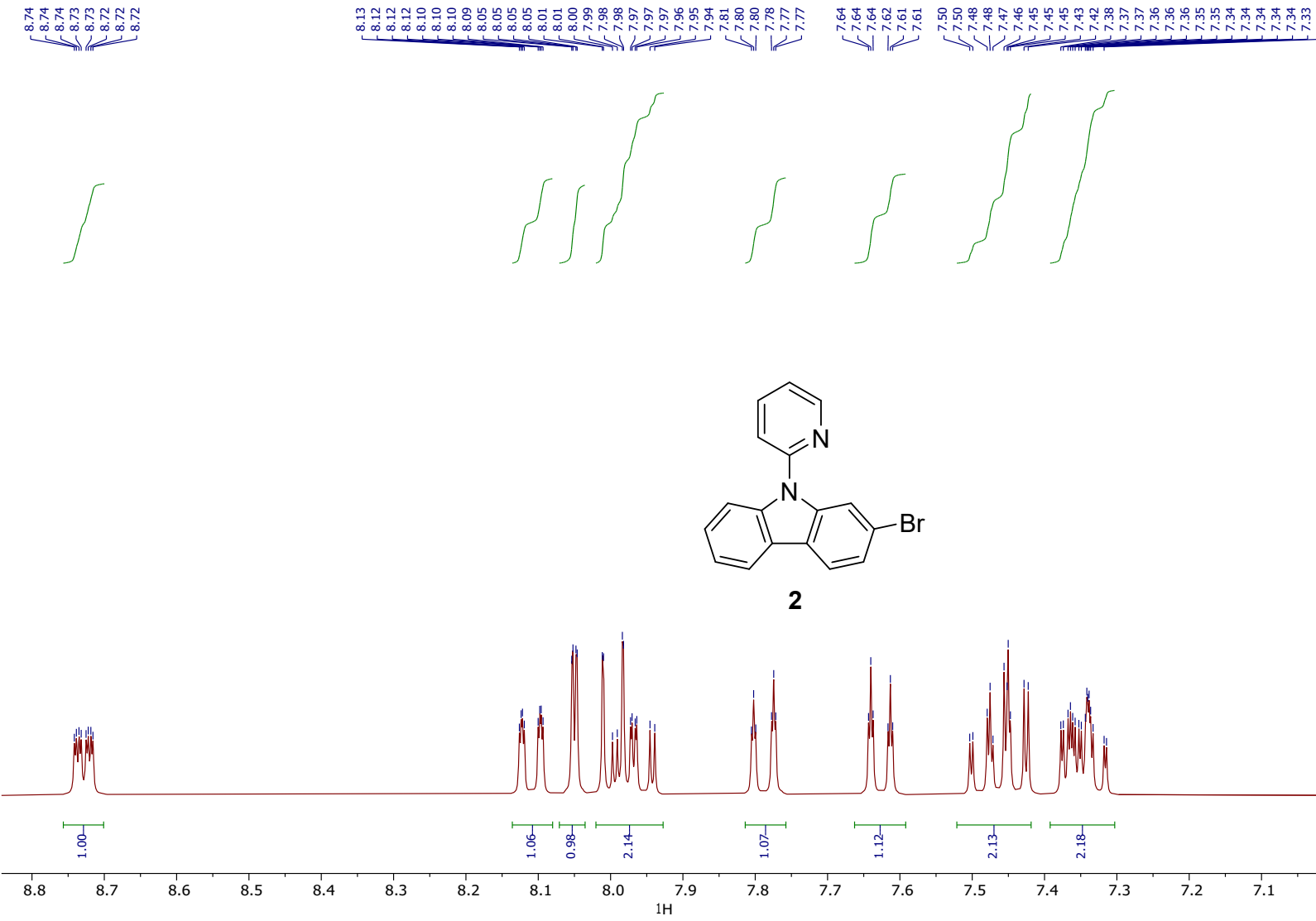


Figure S 22 ¹H-NMR of **2** in CD₂Cl₂

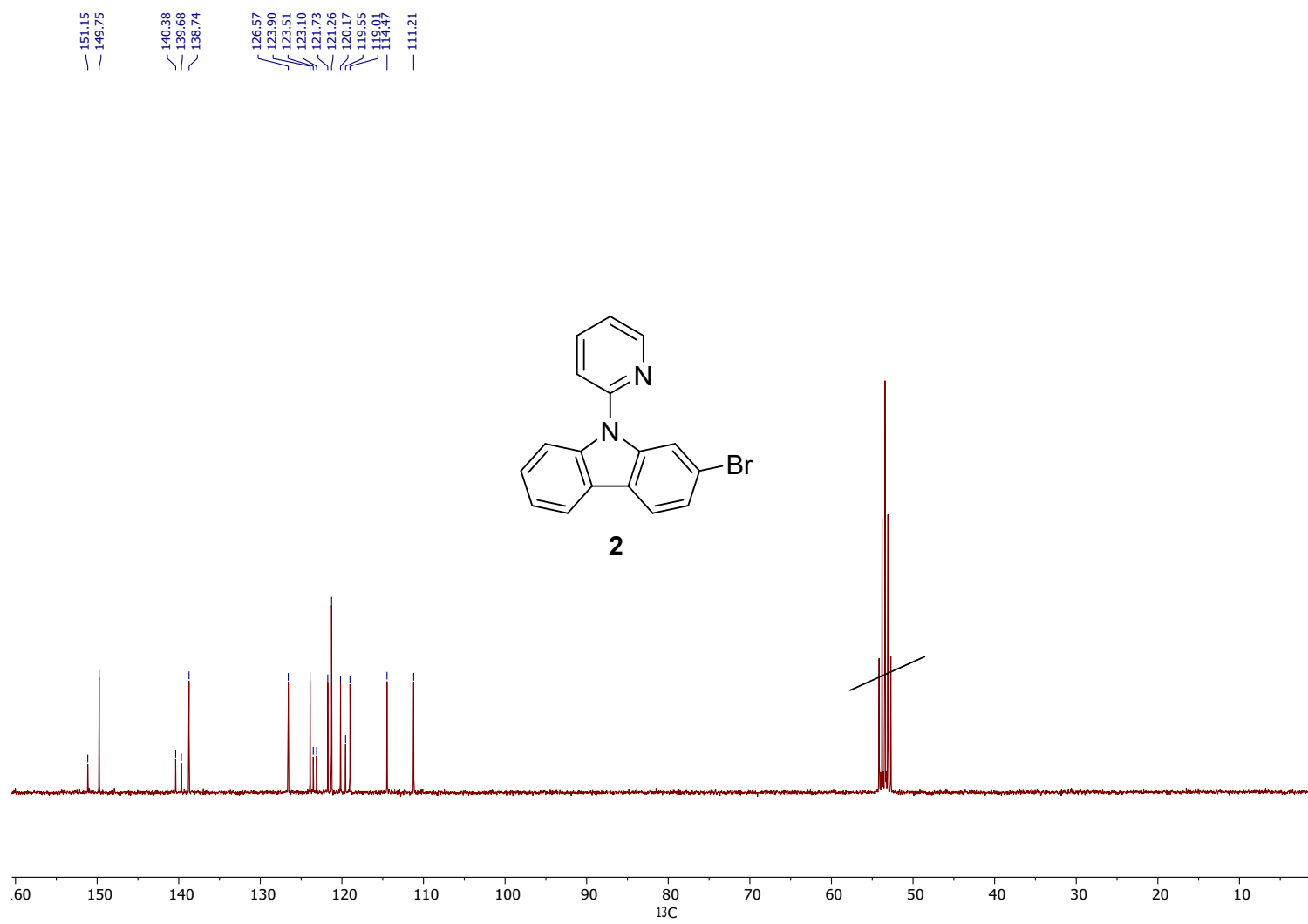


Figure S 23 ^{13}C -NMR of **2** in CD_2Cl_2

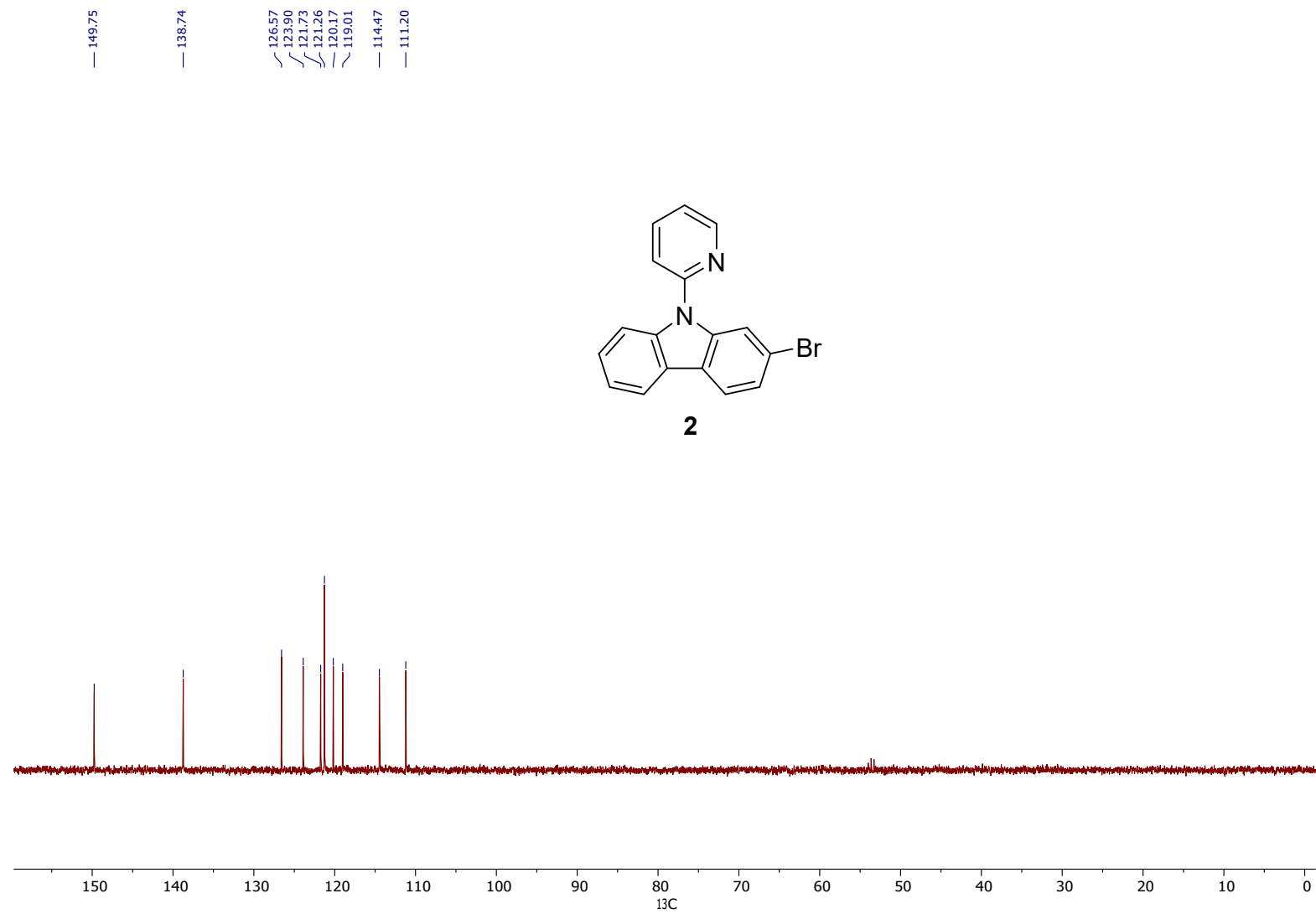


Figure S 24 DEPT-135 of **2** in CD_2Cl_2

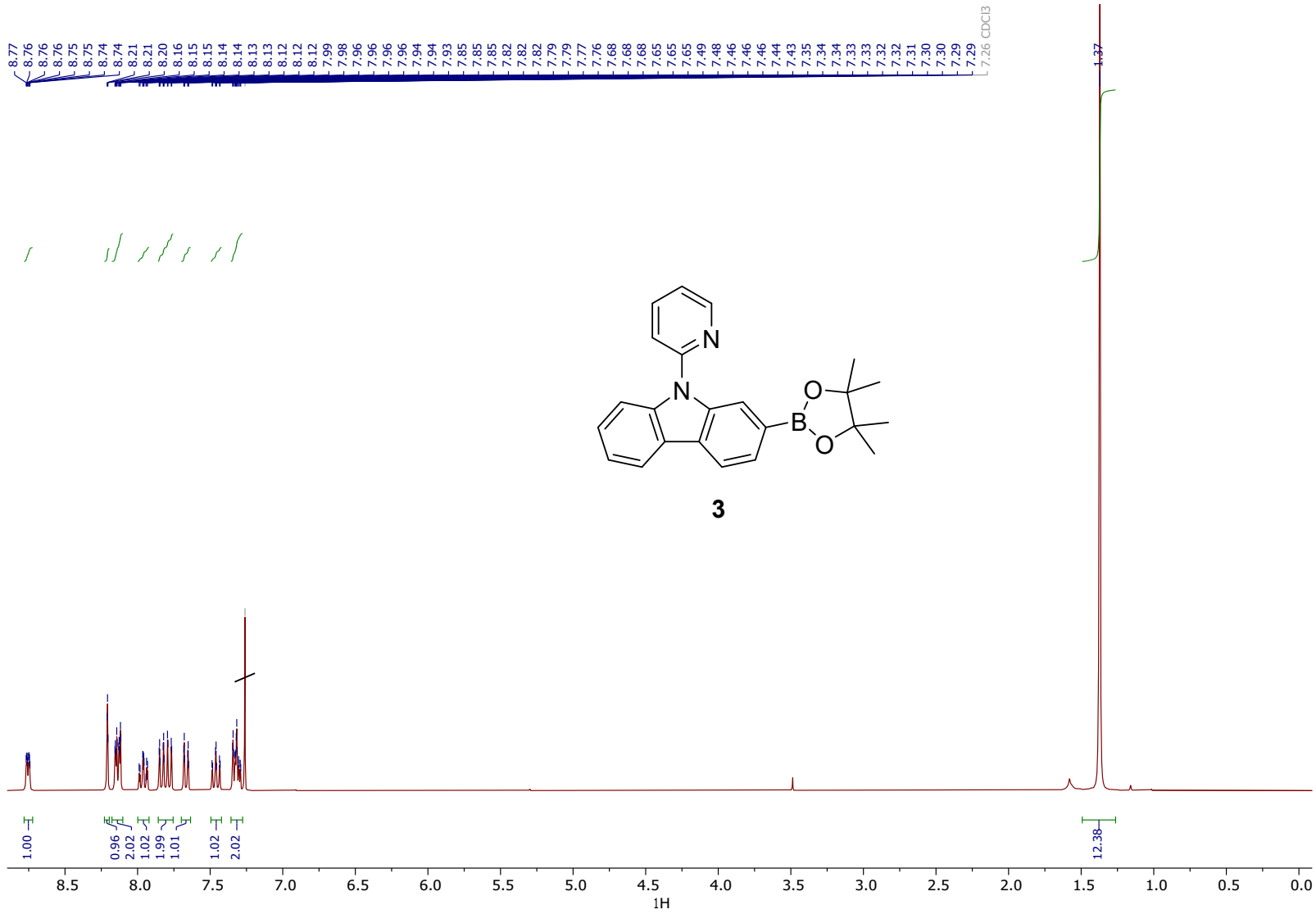


Figure S 25 ^1H -NMR of **3** in CDCl_3

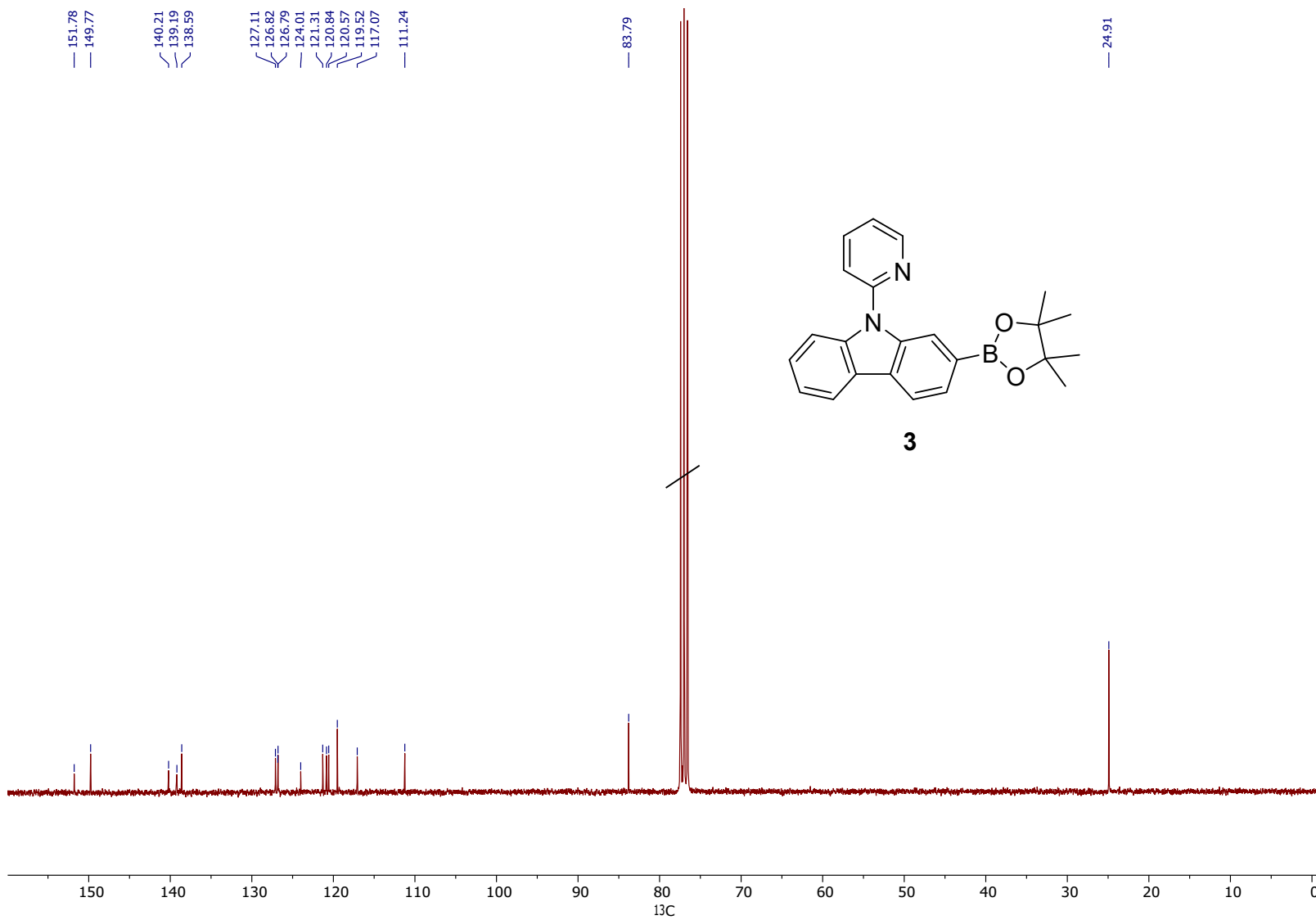


Figure S 26 ^{13}C -NMR of **3** in CDCl_3

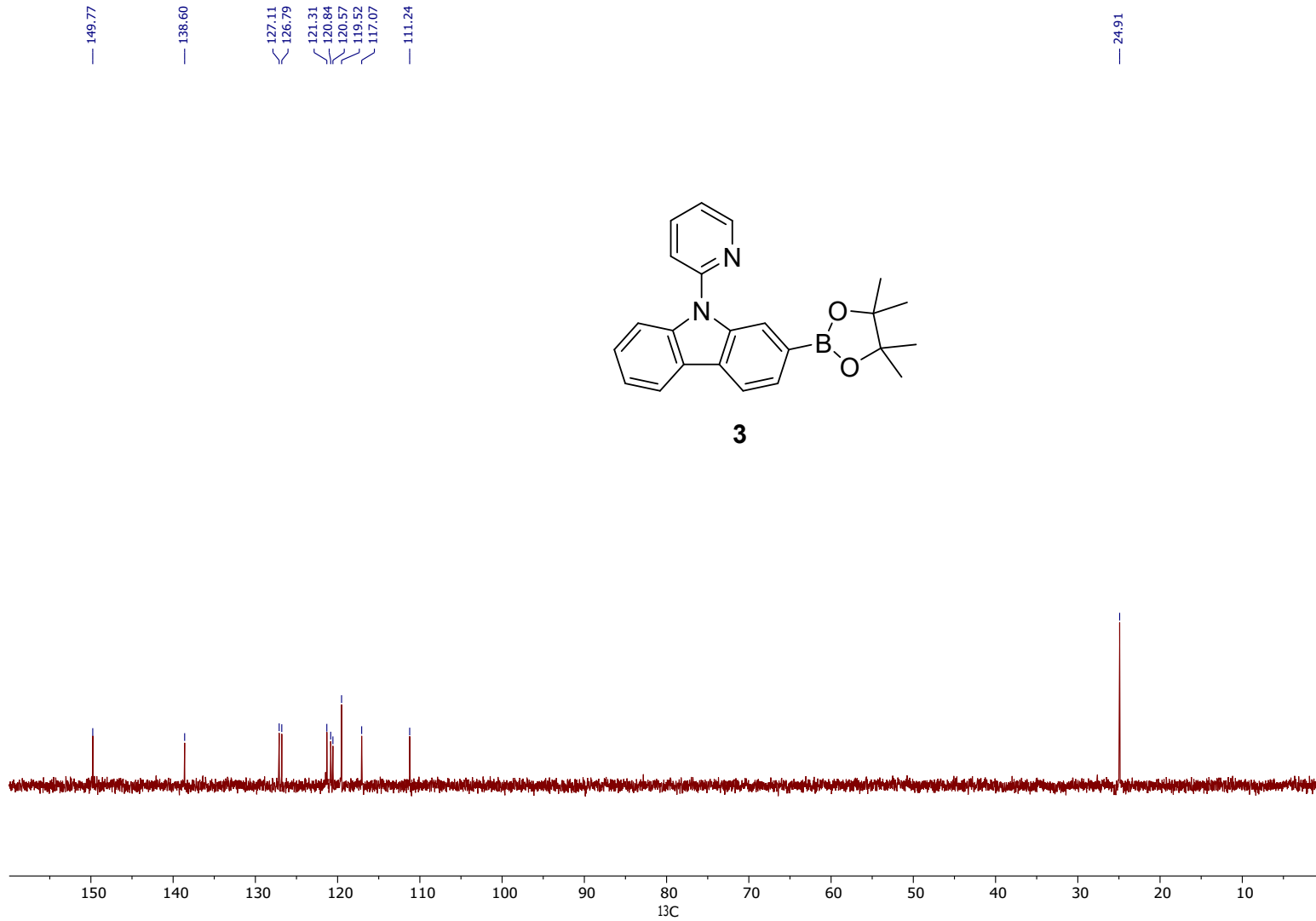


Figure S 27 DEPT 135 of **3** in CDCl_3

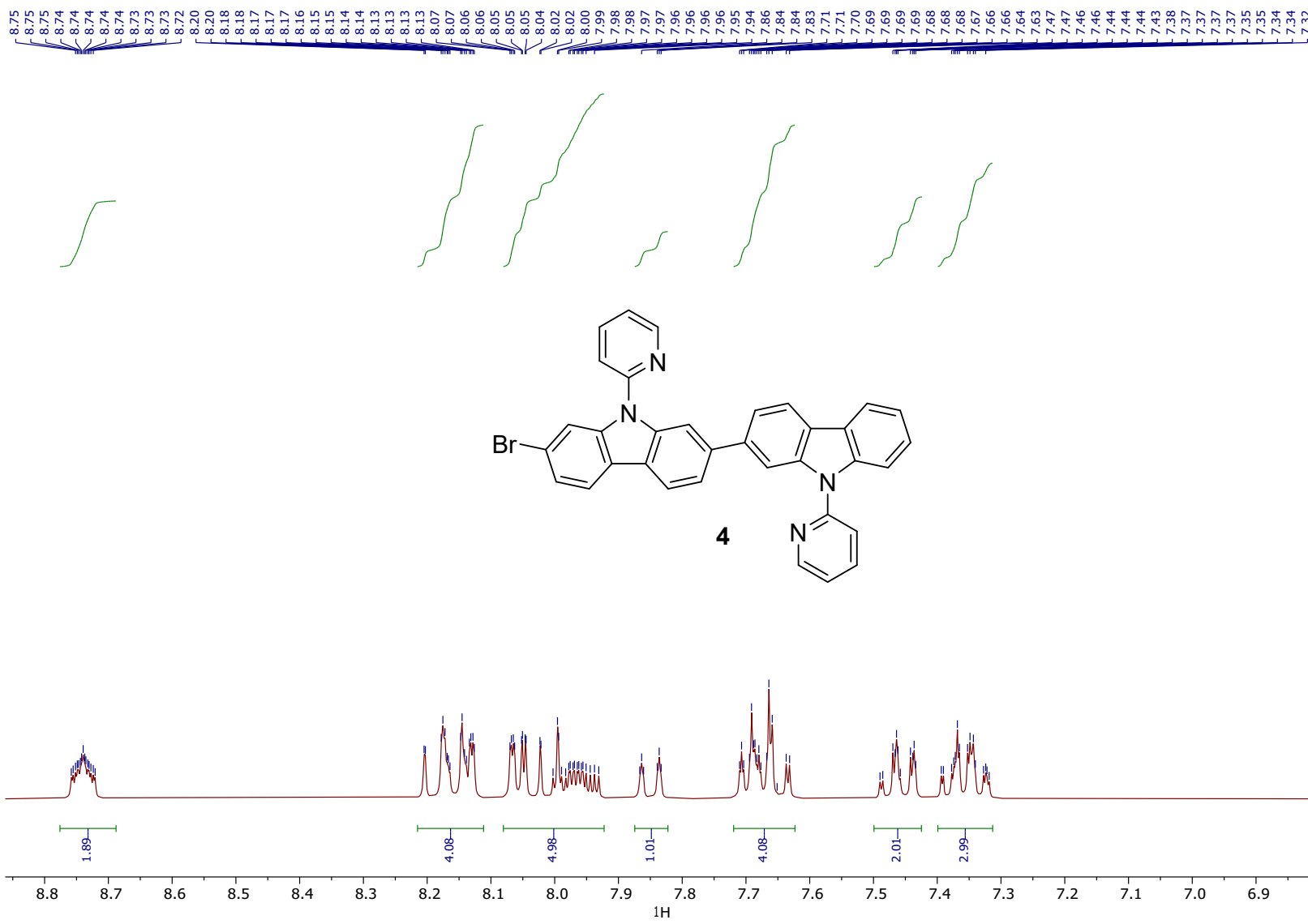


Figure S 28. ^1H NMR of **4** in CD_2Cl_2

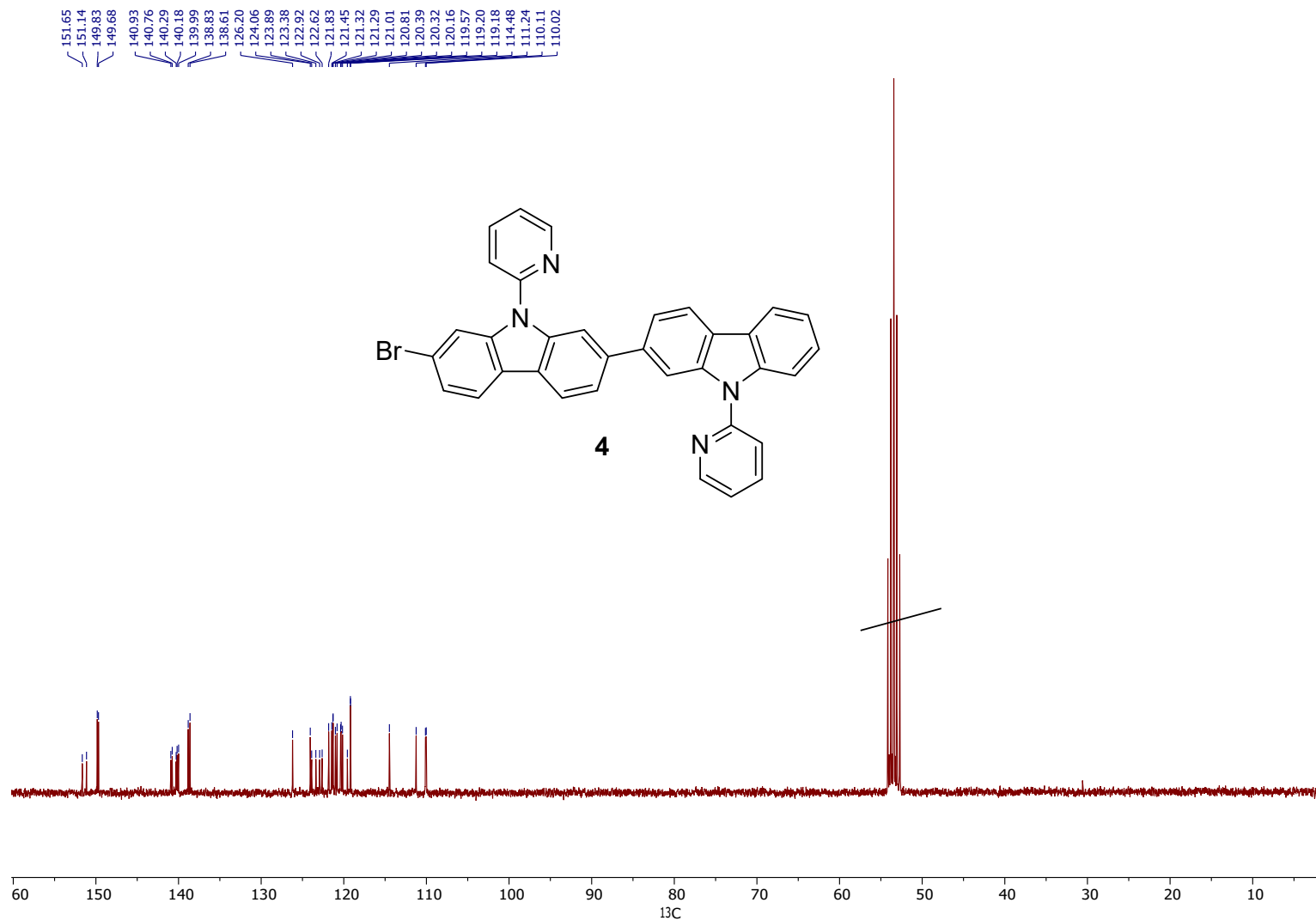


Figure S 29. ^{13}C NMR of **4** in CD_2Cl_2

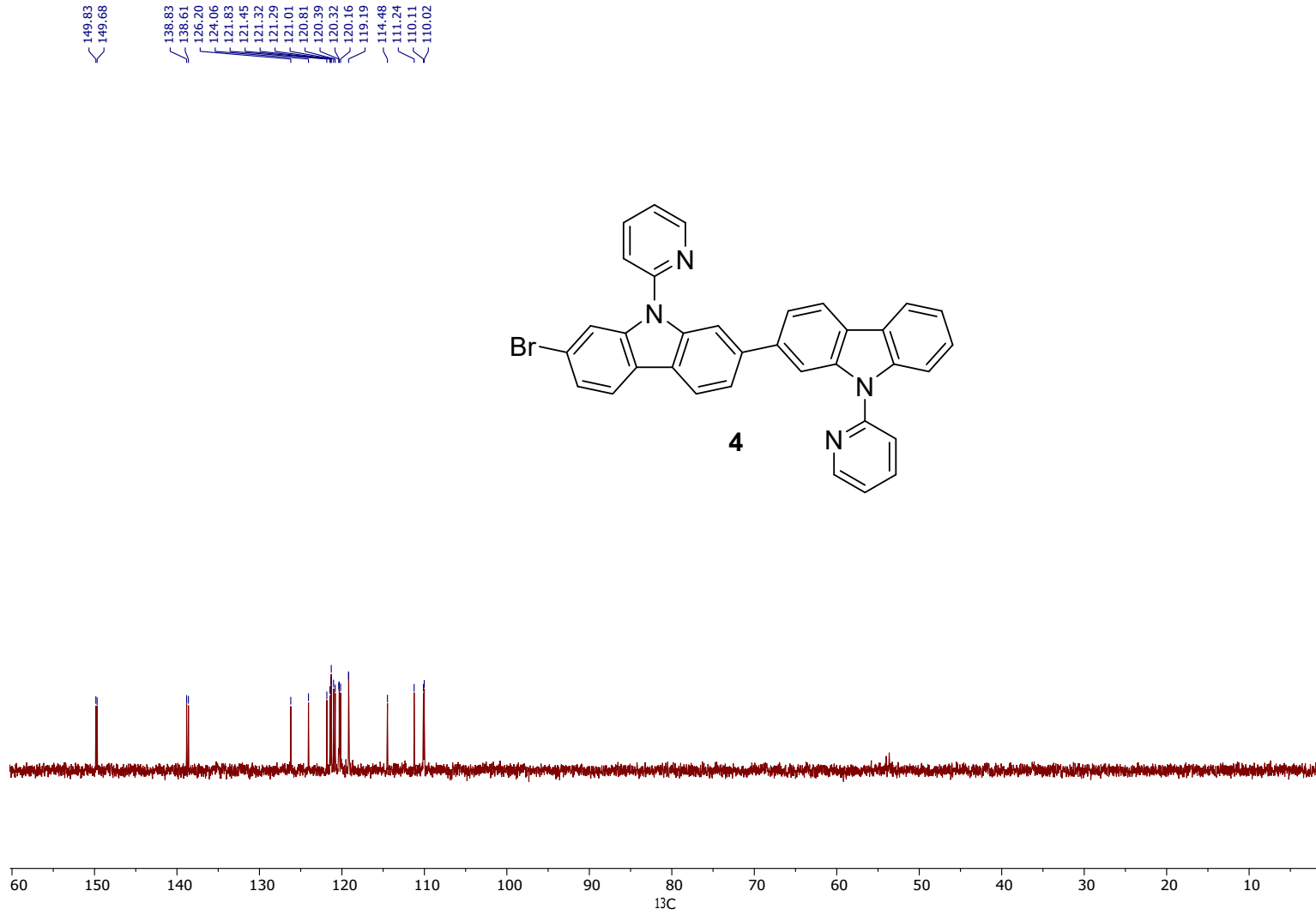


Figure S30. DEPT135 of **4** in CD_2Cl_2

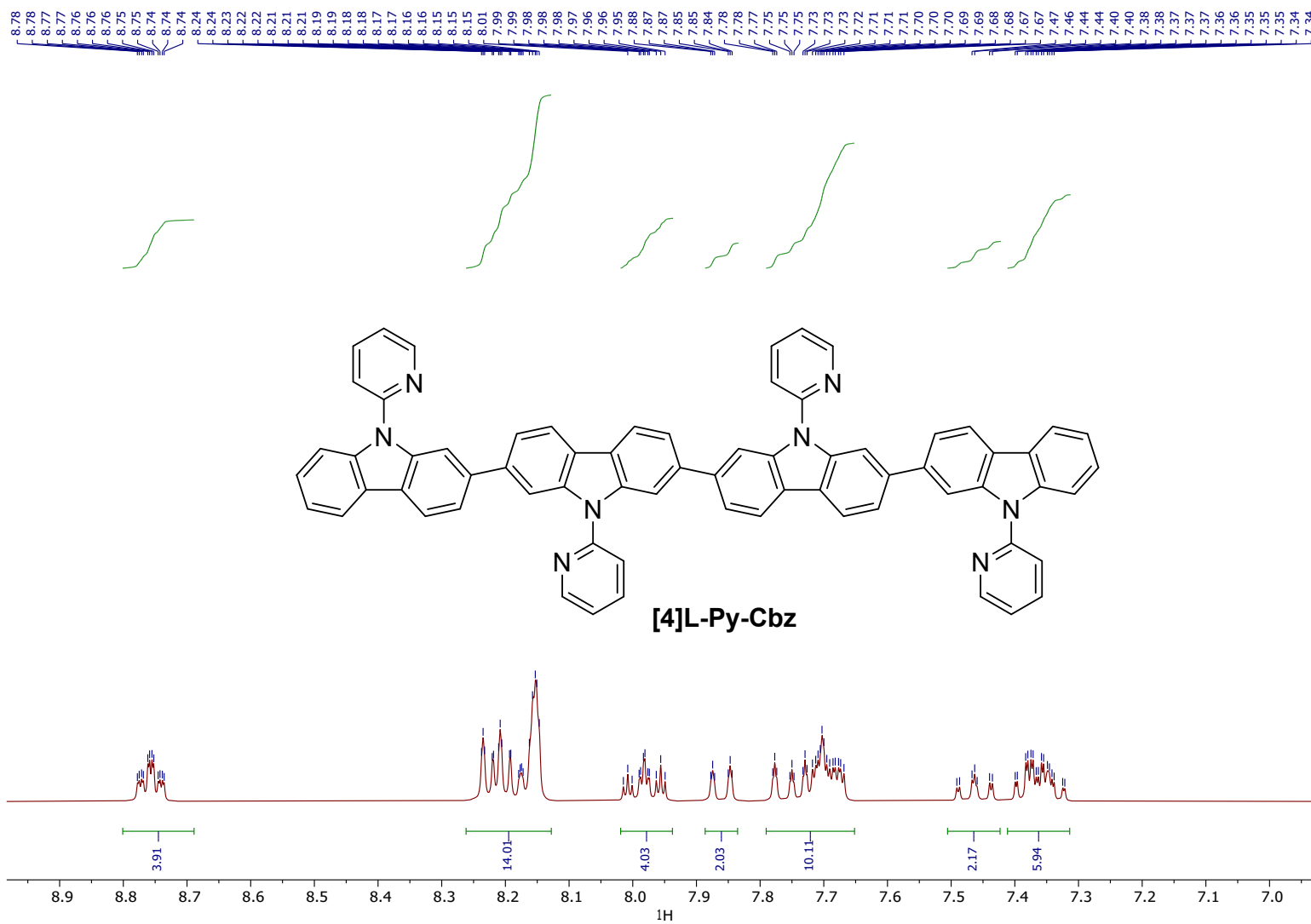


Figure S 31 ^1H NMR of [4]L-Py-Cbz in CD_2Cl_2

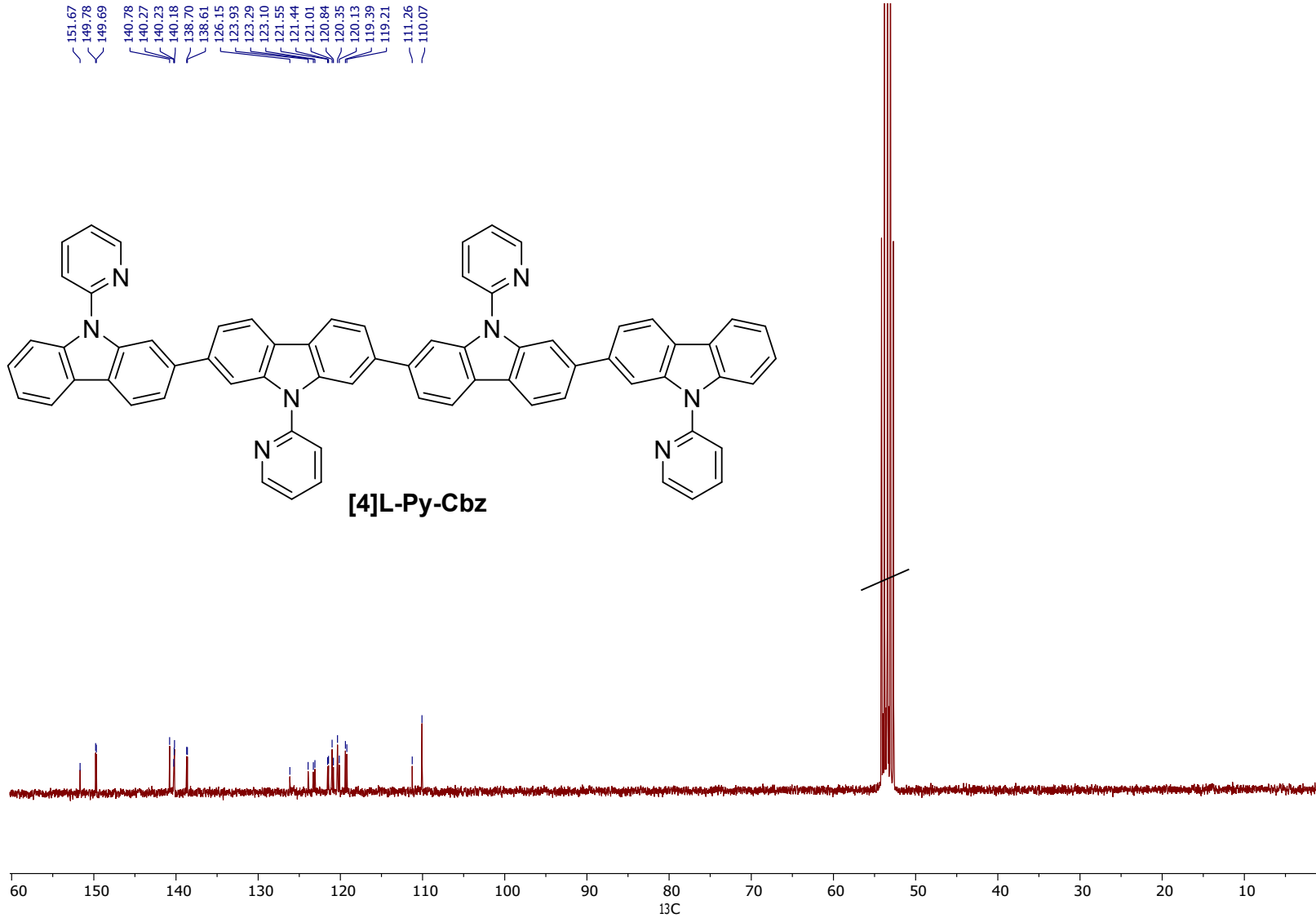


Figure S 32 ^{13}C NMR of [4]L-Py-Cbz in CD_2Cl_2

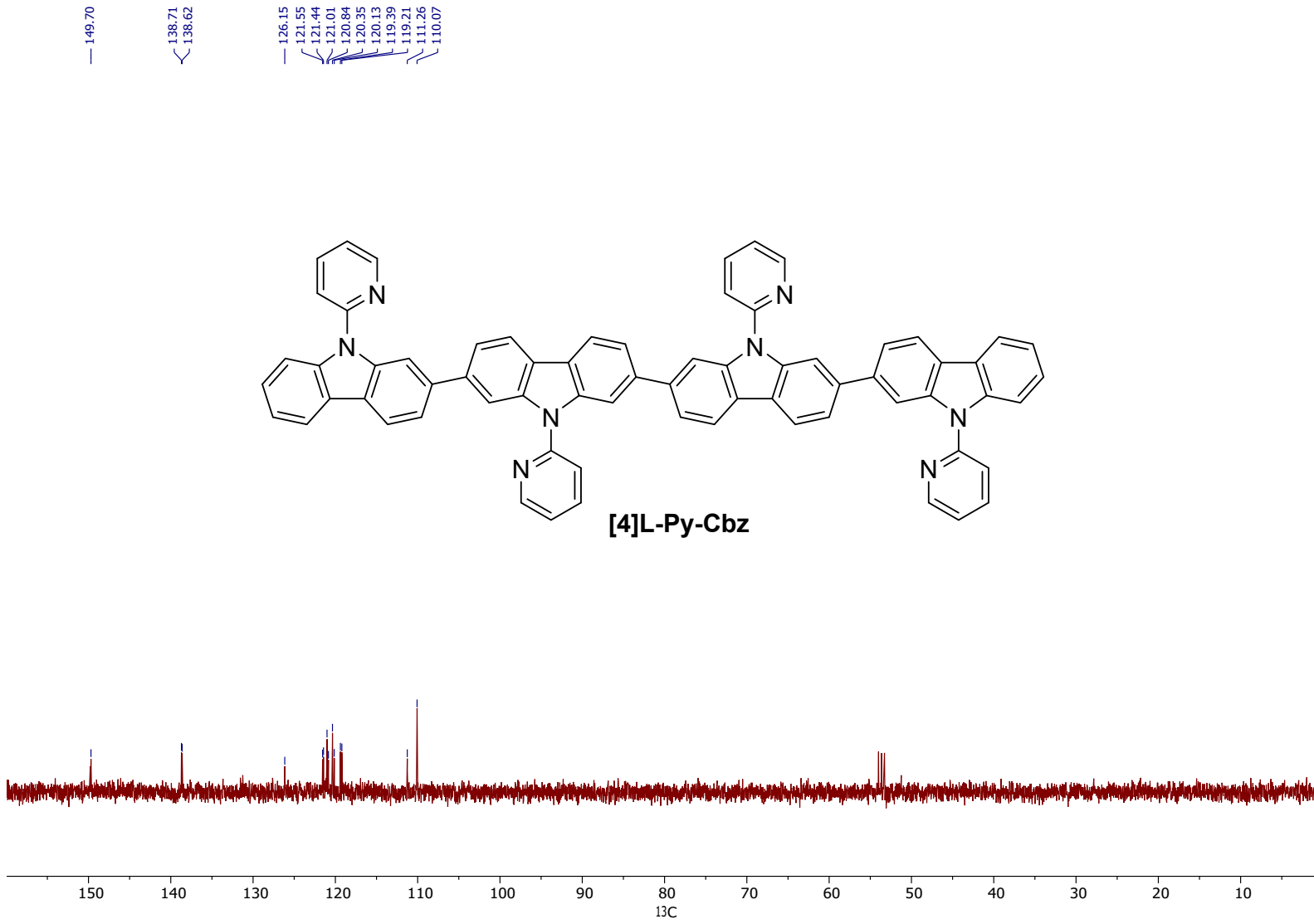


Figure S 33 DEPT135 of [4]L-Py-Cbz in CD_2Cl_2

12 Copy of mass spectra

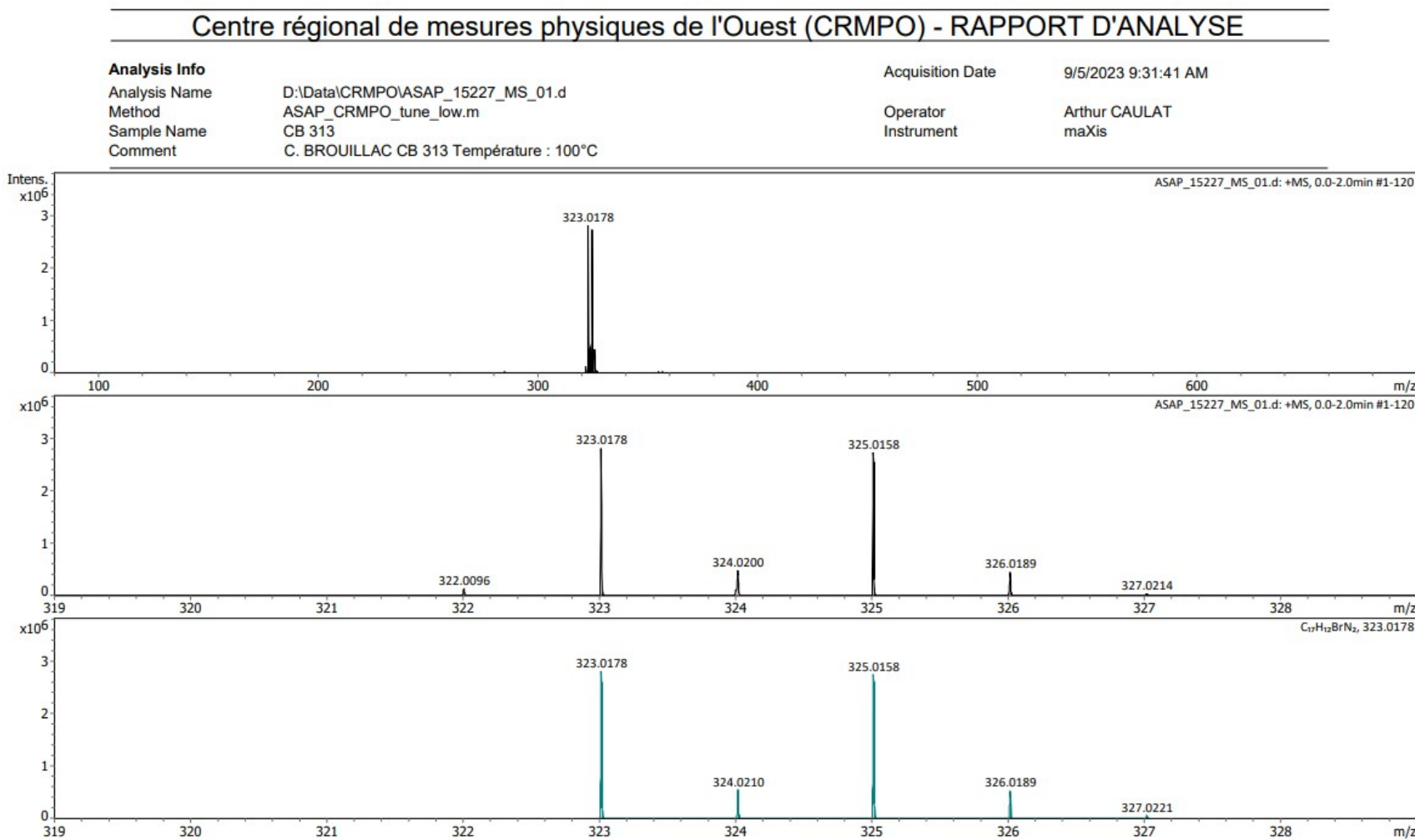


Figure S34 HRMS spectra of 2

Centre régional de mesures physiques de l'Ouest (CRMPO) - RAPPORT D'ANALYSE

Analysis Info

Analysis Name D:\Data\CRMPO\ASAP_15230_MS_02.d
 Method ASAP_CRMPO_tune_low.m
 Sample Name CB 327
 Comment C. BROUILLAC CB 327 Température : 230°C

Acquisition Date 9/5/2023 2:44:47 PM

Operator Arthur CAULAT
 Instrument maXis

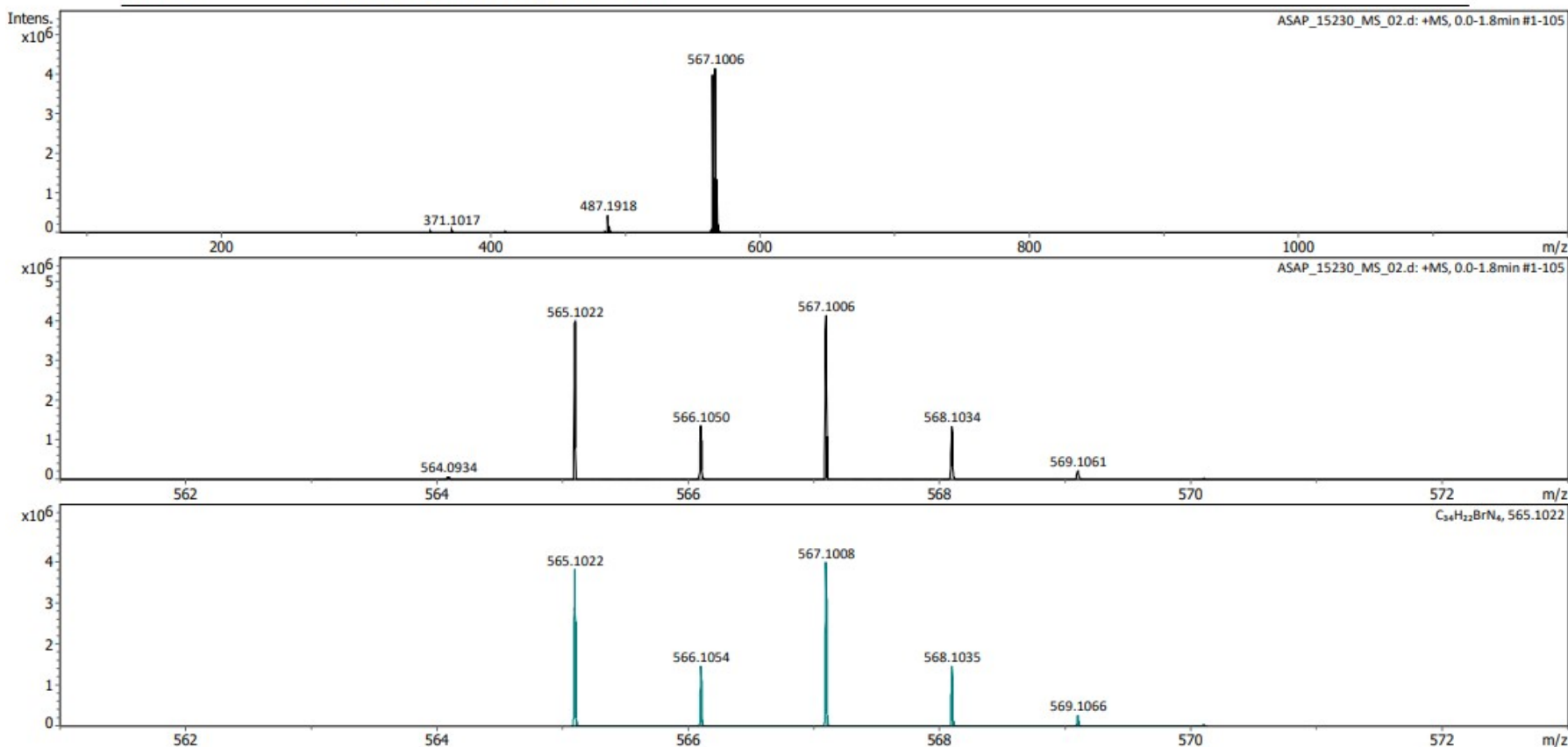
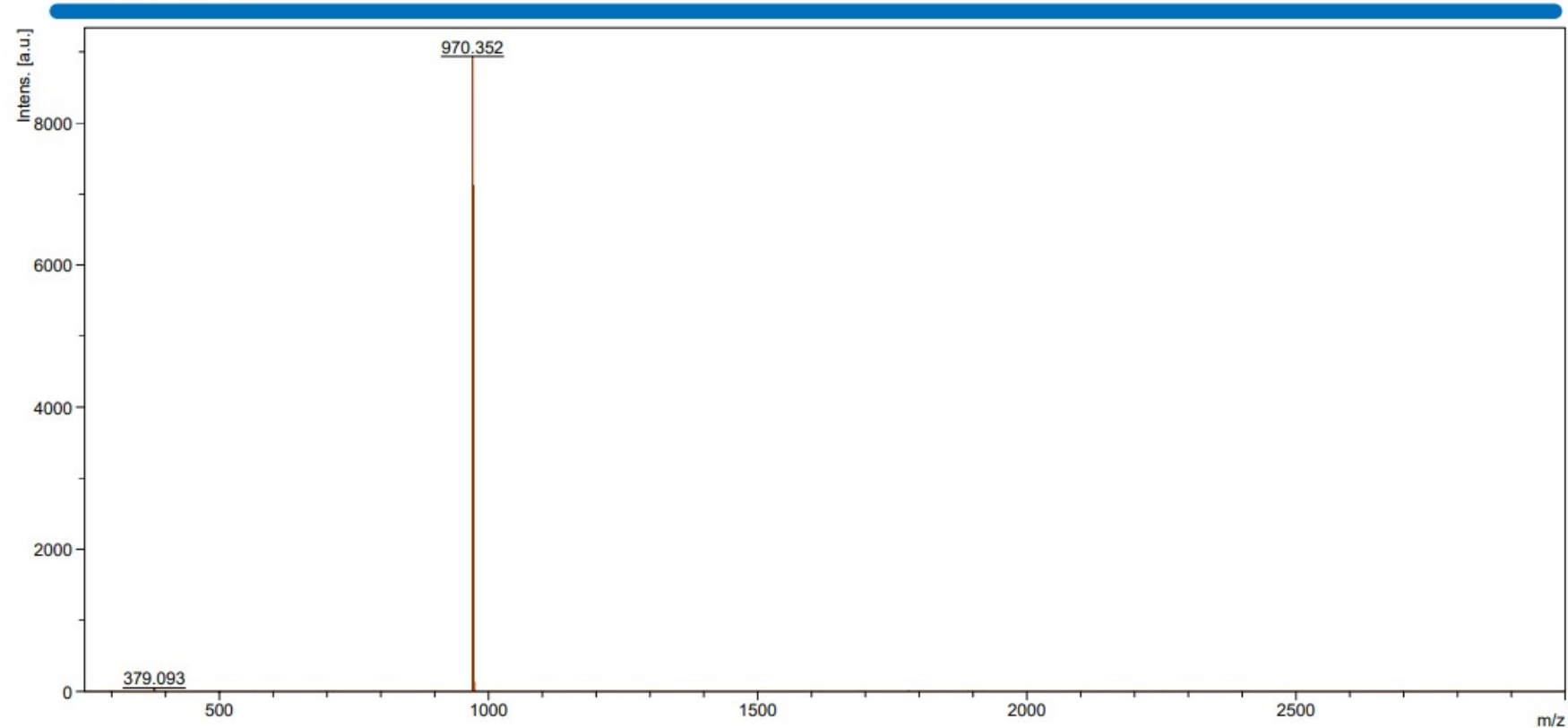


Figure S 35 HRMS spectra of 4

Centre régional de mesures physiques de l'Ouest (CRMPO) - RAPPORT D'ANALYSE

C. BROUILLAC CB 341



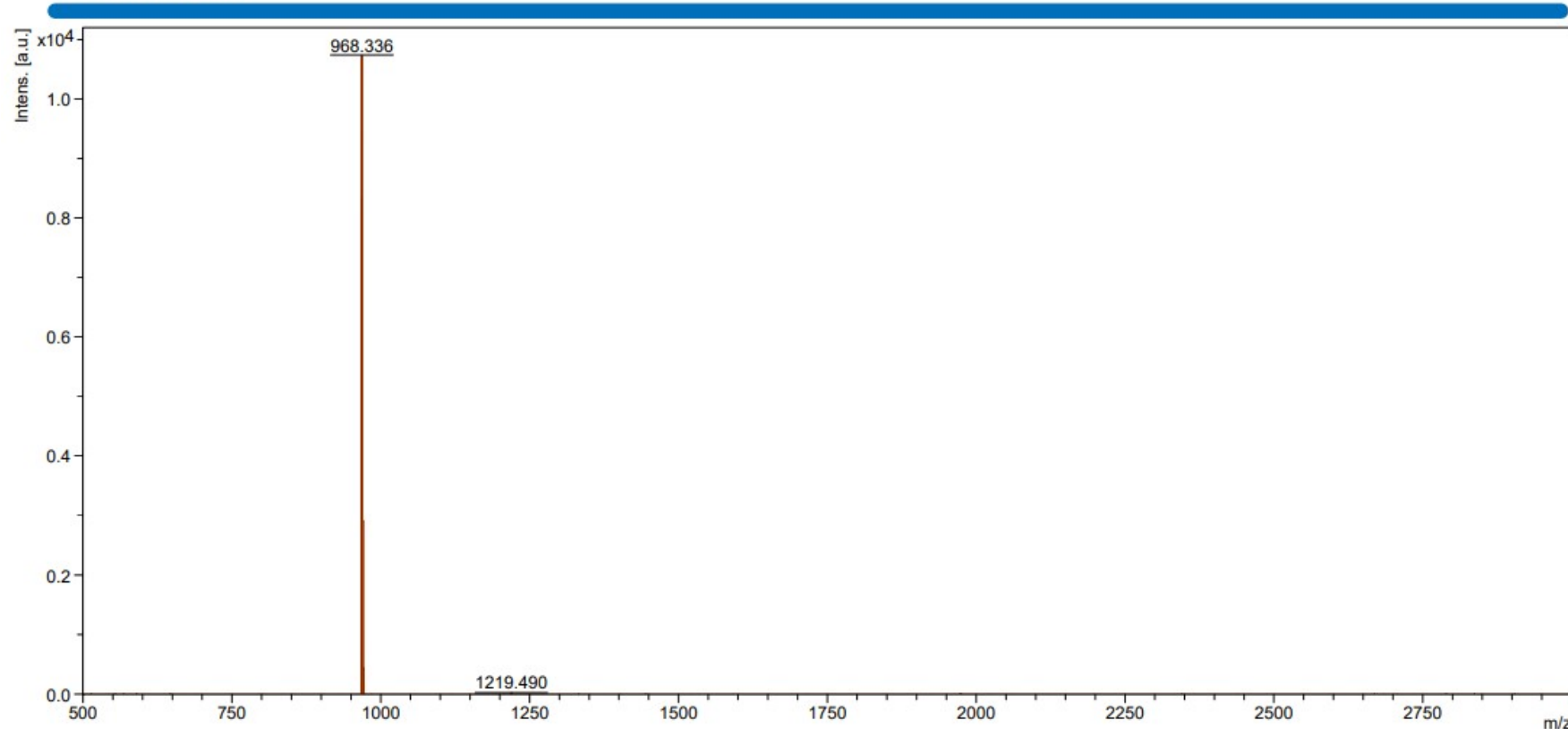
Date of Acquisition 2023-09-05T17:46:08.839+02:00
Acquisition method D:\Methods\flexControlMethods\RP_PepMix.par
Processing method Matrice : DCTB
File Name D:\Data\CRMPO\MALDI_15231_MS_01\0_A13\1

Bruker Daltonics

Figure S36 HRMS spectra of [4]L-Py-Cbz

Centre régional de mesures physiques de l'Ouest (CRMPO) - RAPPORT D'ANALYSE

C. BROUILLAC CB 98



Date of Acquisition 2021-06-25T14:09:29.249+02:00
Acquisition method D:\Methods\flexControlMethods\RP_PepMix.par
Processing method Matrice : DCTB
File Name D:\Data\CRMPO\MALDI_12495_MS_01\0_D14\1

Bruker Daltonics

Figure S37 HRMS spectra of [4]C-Py-Cbz

13 References

- 1 Fulmer, G. R., Miller, A. J. M., Sherden, N. H., Gottlieb, H. E., Nudelman, A., Stoltz, B. M., Bercaw, J. E. & Goldberg, K. I. *Organometallics* **2010**, 2176-2179, 29.
- 2 Altomare, A., Cascarano, G., Giacovazzo, C., Guagliardi, A., Burla, M. C., Polidori, G. & Camalli, M. *J. Appl. Cryst.* **1994**, 435-435, 27.
- 3 Sheldrick, G. *Acta Cryst. C* **2015**, 3-8, 71.
- 4 Farrugia, L. *J. Appl. Cryst.* **2012**, 849-854, 45.
- 5 Kulkarni, A. P., Tonzola, C. J., Babel, A. & Jenekhe, S. A. *Chem. Mater.* **2004**, 4556-4573, 16.
- 6 Iwamoto, T., Watanabe, Y., Sakamoto, Y., Suzuki, T. & Yamago, S. *J. Am. Chem. Soc.* **2011**, 8354-8361, 133.
- 7 Brouillac, C., McIntosh, N., Heinrich, B., Jeannin, O., De Sagazan, O., Coulon, N., Rault-Berthelot, J., Cornil, J., Jacques, E., Quinton, C. & Poriel, C. *Adv. Sci.* **2024**, 2309115.
- 8 Li, G., Shen, G., Fang, X., Yang, Y.-F., Zhan, F., Zheng, J., Lou, W., Zhang, Q. & She, Y. *Inorg. Chem.* **2020**, 18109-18121, 59.
- 1 Fulmer, G. R., Miller, A. J. M., Sherden, N. H., Gottlieb, H. E., Nudelman, A., Stoltz, B. M., Bercaw, J. E. & Goldberg, K. I. *Organometallics* **2010**, 2176-2179, 29.
- 2 Kulkarni, A. P., Tonzola, C. J., Babel, A. & Jenekhe, S. A. *Chem. Mater.* **2004**, 4556-4573, 16.
- 3 Iwamoto, T., Watanabe, Y., Sakamoto, Y., Suzuki, T. & Yamago, S. *J. Am. Chem. Soc.* **2011**, 8354-8361, 133.
- 4 Brouillac, C., McIntosh, N., Heinrich, B., Jeannin, O., De Sagazan, O., Coulon, N., Rault-Berthelot, J., Cornil, J., Jacques, E., Quinton, C. & Poriel, C. *Adv. Sci.* **2024**, 2309115.
- 5 Li, G., Shen, G., Fang, X., Yang, Y.-F., Zhan, F., Zheng, J., Lou, W., Zhang, Q. & She, Y. *Inorg. Chem.* **2020**, 18109-18121, 59.